J|A|C|S
ARTICLES
Published on Web 01/09/2003

Impact of Azaproline on Amide Cis−Trans Isomerism: Conformational Analyses and NMR Studies of Model Peptides Including TRH Analogues

Wei-Jun Zhang,[†] Anders Berglund,[†,||] Jeff L.-F. Kao,[‡] Jean-Pierre Couty,[§] Marvin C. Gershengorn,[§] and Garland R. Marshall*[,†]

Contribution from the Departments of Biochemistry and Molecular Biophysics and of Chemistry, Washington University, St. Louis, Missouri 63110, and Division of Molecular Medicine, Department of Medicine, Weil Medical College of Cornell University, New York, New York 10021

Received July 19, 2002; E-mail: garland@pcg.wustl.edu

Abstract: The β-turn is a well-studied motif in both proteins and peptides. Four residues, making almost a complete 180°-turn in the direction of the peptide chain, define the β-turn. Several types of the β-turn are defined according to Φ and Ψ torsional angles of the backbone for residues $i+1$ and $i+2$. One special type of β-turn, the type VI-turn, usually contains a proline with a *cis*-amide bond at residue $i+2$. In an aza-amino acid, the α-carbon of the amino acid is changed to nitrogen. Peptides containing azaproline (azPro) have been shown to prefer the type VI β-turn both in crystals and in organic solvents by NMR studies. MC/MD simulations using the GB/SA solvation model for water explored the conformational preferences of azPro-containing peptides in aqueous systems. An increase in the conformational preference for the *cis*-amide conformer of azPro was clearly seen, but the increased stability was relatively minor with respect to the *trans*-conformer as compared to previous suggestions. To test the validity of the calculations in view of the experimental data from crystal structures and NMR in organic solvents, [azPro^3]-TRH and [Phe^2, azPro^3]-TRH were synthesized, and their conformational preferences were determined by NMR in polar solvents as well as the impact of the azPro substitution on their biological activities.

Introduction

The β-turn is a well-studied motif in both proteins and cyclic peptides (for reviews, see Rose et al.[1] or Richardson[2]). Four sequential residues, making an almost complete 180°-turn in the direction of the peptide chain, define a reverse turn, the most rigorously defined subset of which is the β-turn. There are several types of β-turns as described in the literature usually requiring an internal hydrogen bond between residues one and four.[3,4] The different types are defined according to the Φ- and Ψ-backbone torsional angles for residues 2 and 3. One special type of β-turn is the type VI-turn defined by a proline with a *cis*-amide bond located at residue 3. Richardson[2] divided this class into two different subclasses, type VIa and VIb. Type VIa usually has an internal hydrogen bond, while type VIb does not usually make a hydrogen bond. The reported values for (Φ_2, Ψ_2), (Φ_3, Ψ_3) torsions for the two types of VI-turns are as follow:[1]

type VIa: ($\Phi_2 = -60°$, $\Psi_2 = 120°$), ($\Phi_3 = -90°$, $\Psi_3 = 0°$)

type VIb: ($\Phi_2 = -120°$, $\Psi_2 = 120°$), ($\Phi_3 = -60°$, $\Psi_3 = 0°$)

The conformational space for a set of tripeptides containing a *cis*-amide bond was studied by Nagarajaram et al.,[5] who reported the minimum-energy conformation for a set of Xxx-*cis*-Pro combinations including Ala-Pro and Pro-Pro. These studies also ruled out the occurrence of a *cis*-amide bond for the first proline in Pro-*cis*-Pro due to its high energy. Two different types of hydrogen bond were found, type 4 → 1 and type 1 → 2. There is a high degree of the *cis*-amide conformer of proline observed in peptides and proteins; the intrinsic probability for a *cis*-amide bond instead of the *trans*-conformation of the amide bond preceding a proline is 0.1−0.3 as compared to less than 10^{-3} for the rest of the amino acids.[6] The energy barrier for cis−trans isomerization is also less for proline as compared to those of the rest of the amino acids. One reason of this is the greater length of the Xxx−Pro bond, 1.36 Å for proline as compared to 1.33 Å for the usual amide bond. This comes from the loss of the amide hydrogen resulting

[†] Department of Biochemistry and Molecular Biophysics, Washington University.
[‡] Department of Chemistry, Washington University.
[§] Weil Medical College of Cornell University.
[||] Current address: Research Group for Chemometrics, Department of Chemistry, Umeå University, S-901 87 Umeå, Sweden.

(1) Rose, G. D.; Gierasch, L. M.; Smith, J. A. *Adv. Protein Chem.* **1985**, *37*, 1−109.
(2) Richardson, J. S. *Adv. Protein Chem.* **1981**, *34*, 167−339.
(3) Venkatachalam, C. M. *Biopolymers* **1968**, *6*, 1425−1436.
(4) Lewis, P. N.; Momany, F. A.; Scheraga, H. A. *Biochim. Biophys. Acta* **1973**, *303*, 211−229.
(5) Nagarajaram, H. A.; Paul, P. K. C.; Ramanarayanan, K.; Soman, K. V.; Ramakrishnan, C. *Int. J. Pept. Protein Res.* **1992**, *40*, 383−394.
(6) Brandts, J. F.; R., H. H.; Brennan, M. *Biochemistry* **1975**, *14*, 4953−4963.

in a lack of resonance stabilizing and a redistribution of charge. Jorgensen and Gao[7] and Ciepak and Kollman[8] have explored the relative stabilities of *cis*−*trans*-amide conformers of *N*-methylacetamide by ab initio calculations and molecular simulations in the gas phase and in aqueous solution.

There are many examples of how the peptide backbone can be modified to help stabilize a desired conformation. We have previously studied the conformational space for the Pro-D-NMe-amino acid sequence[9] and also the effect of N-methylation and N-hydroxylation[10] on reverse-turn stabilization. Backbone conformations can be stabilized by incorporation of many different modified amino acids and dipeptides (see Lubell[11,12] and references therein). Another, less investigated, modification is the aza-amino acid. In an aza-amino acid, the α-carbon is changed to nitrogen; this definition precedes that of Mish et al.,[13] who referred to the Δ^2-pyrazoline-5-carboxylic acids obtained by cycloaddition as azaproline. Azapeptides contain aza-amino acids, and numerous aza-analogues of biologically active peptides have been prepared, for example, angiotensin II,[14] oxytocin,[15] eledoisin,[16] enkephalin,[17] and luliberin (LHRH)[18,19] with one analogue [D-Ser(*t*-Bu),[6] azGly[10]]-LHRH, a commercial product, Zoladex, ICI 118630, for the treatment of prostate carcinoma. More recently, azaglycine has been studied as a replacement for the central residue of the RGD recognition motif of integrins.[20,21] The azapeptide linkage also appears to confer resistant to degradation by many proteolytic enzymes as originally discovered by Oehme et al.[22] and Dutta and Giles.[23] The azapeptide linkage has been incorporated into inhibitors of various enzymes, such as angiotensin converting enzyme,[24] cysteine protease,[25,26] renin,[27] human leukocyte elastase,[28] and human rhinovirus 3C protease.[29] A promising new HIV protease inhibitor atazanavir (BMS-232632) contains a *para*-substituted azaphenylalanine and is active against multiple-resistant strains.[30]

A special example of azapeptides is the azatide that is defined as a "pure azapeptide", where the α-carbon for each amino acid is changed to nitrogen.[31,32] An inhibitor of renin prepared by Gante et al.[27] was the first example of a biologically active azatide.

Lee et al.[33] studied by ab initio calculations the structural perturbation introduced into formyl-amino acid-amides by changing the α-carbon to nitrogen. The global minimum energy conformation for these compounds (azGly, AzAla, AzLeu) suggested a β-turn motif with the aza residue at the $i + 2$nd position. The peptide Boc-Phe-azLeu-Ala-OMe was prepared, and its structural preference was determined in organic solvents. The data supported a type II β-turn as predicted. More relevant to this study, azapeptides containing azaproline (azPro) have been shown to prefer the β-turn type VI in crystals[34,35] and also by NMR studies[36] in organic solvents. The two adjacent nitrogens in the ring show a clear pyramidal character in the reported crystal structures. The amide bond is also longer, giving a lower barrier for the cis−trans isomerization. This finding is also supported by a theoretical study of diformylhydrazine by Reynolds at al.[37] The calculations are focused on the *Z*,*Z*, *Z*,*E*, and *E*,*E* conformations of diformylhydrazine as well as the rotational barrier for the CO−N−N−CO torsional angle. In these calculations, the two nitrogens had a pyramidal conformation for all of the conformations. The fact that diformylhydrazine has a flat conformation in crystal structures is probably due to crystal packing forces in that a planar conformation allows stacked sheets of hydrogen-bonded networks. Aza-amino acids have also been used in the backbone in a peptide/oligourea/azapeptide hybrid for inducing a hairpin turn.[38]

The focus of this paper is the quantitative determination both computationally and experimentally of the conformational influence of azaproline (azPro) in stabilizing reverse-turn conformations in peptides. The previous observations[34−36] that the enhanced *cis*-amide conformation was induced by azPro increased the probability of type VI reverse-turns. Analogues of thyrotropin-releasing hormone (TRH) containing azPro were included to further probe the receptor-bound conformation of TRH. TRH is a natural tripeptide, L-pyroglutamyl-L-histidyl-L-proline-amide (pGlu-His-Pro-NH_2), a prominent neuromessenger released from the hypothalamus that controls the release of thyroid stimulating hormone (TSH) from the pituitary. Several papers have investigated the solution conformation of TRH[39−42] in the hopes of gaining insight into the biologically relevant conformation. One study has shown that the activity is correlated

(7) Jorgensen, W. L.; Gao, J. *J. Am. Chem. Soc.* **1988**, *110*, 4212−4216.
(8) Cieplak, P.; Kollman, P. *J. Comput. Chem.* **1991**, *12*, 1222−1236.
(9) Chalmers, D. K.; Marshall, G. R. *J. Am. Chem. Soc.* **1995**, *117*, 5927−5937.
(10) Takeuchi, Y.; Marshall, G. R. *J. Am. Chem. Soc.* **1998**, *120*, 5363−5372.
(11) Hanessian, S.; McNaughton-Smith, G.; Lombart, H.-G.; Lubell, W. D. *Tetrahedron* **1997**, *53*, 12789−12854.
(12) Halab, L.; Lubell, W. D. *J. Org. Chem.* **1999**, *64*, 3312−3321.
(13) Mish, M. R.; Guerra, F. M.; Carreira, E. M. *J. Am. Chem. Soc.* **1997**, *119*, 8379−8380.
(14) Hess, H.-J.; Moreland, W. T.; Laubach, G. D. *J. Am. Chem. Soc.* **1963**, *85*, 4041.
(15) Niedrich, H. *J. Prakt. Chem.* **1972**, *314*, 769.
(16) Oehme, P.; Bergmann, J.; Falck, M.; Reich, J. G.; Vogt, W. E.; Niedrich, H.; Pirrwitz, J.; Berseck, C.; Jung, F. *Acta Biol. Med. Germanica* **1972**, *28*, 109−120.
(17) Han, H.; Yoon, J.; Janda, K. D. *Bioorg. Med. Chem. Lett.* **1998**, *8*, 117−120.
(18) Dutta, A. S.; Furr, B. J.; Giles, M. B.; Valcaccia, B. *J. Med. Chem.* **1978**, *21*, 1018−1024.
(19) Dutta, A. S.; Furr, B. J.; Giles, M. B.; Valcaccia, B.; Walpole, A. L. *Biochem. Biophys. Res. Commun.* **1978**, *81*, 382−390.
(20) Gibson, C.; Goodman, S. L.; Hahn, D.; Holzemann, G.; Kessler, H. *J. Org. Chem.* **1999**, *64*, 7388−7394.
(21) Sulyok, G. A.; Gibson, C.; Goodman, S. L.; Holzemann, G.; Wiesner, M.; Kessler, H. *J. Med. Chem.* **2001**, *44*, 1938−1950.
(22) Oehme, P.; Katzwinkel, S.; Vogt, W. E.; Niedrich, E. *Experientia* **1973**, *29*, 947.
(23) Dutta, A. S.; Giles, M. B. *J. Chem. Soc., Perkin Trans. 1* **1976**, 244−248.
(24) Greenlee, W. J.; Thorsett, E. D.; Springer, J. P.; Patchett, A. A. *Biochem. Biophys. Res. Commun.* **1984**, *122*, 791−797.
(25) Magrath, J.; Abeles, R. H. *J. Med. Chem.* **1992**, *35*, 4279−4283.
(26) Xing, R.; Hanzlik, R. P. *J. Med. Chem.* **1998**, *41*, 1344−1351.
(27) Gante, J.; Krug, M.; Lauterbach, G.; Weitzel, R.; Hiller, W. *J. Pept. Sci.* **1995**, *1*, 201−206.
(28) Powers, J. C.; Boone, R.; Carroll, D. L.; Gupton, B. F.; Kam, C. M.; Nishino, N.; Sakamoto, M.; Tuhy, P. M. *J. Biol. Chem.* **1984**, *259*, 4288−4294.
(29) Venkatraman, S.; Kong, J.; Nimkar, S.; Wang, Q. M.; Aube, J.; Hanzlik, R. P. *Bioorg. Med. Chem. Lett.* **1999**, *9*, 577−580.
(30) Witherell, G. *Curr. Opin. Invest. Drugs* **2001**, *2*, 340−347.
(31) Han, H.; Janda, K. D. *J. Am. Chem. Soc.* **1996**, *118*, 2539−2544.
(32) Han, H.; Yoon, J.; Janda, K. D. In *Peptidomimetics Protocols*; Kazmierski, W. M., Ed.; Humana Press: Totowa, NJ, 1998; Vol. 23, Chapter 106, pp 87−102.
(33) Lee, H.-J.; Ahn, I.-A.; Ro, S.; Choi, K.-H.; Choi, Y.-S.; Lee, K.-B. *J. Pept. Res.* **2000**, *56*, 35−46.
(34) Lecoq, A.; Boussard, G.; Marraud, M.; Aubry, A. *Biopolymers* **1993**, *33*, 1051−1059.
(35) Didierjean, C.; Del Duca, V.; Benedetti, E.; Aubry, A.; Zouikri, M.; Marraud, M.; Boussard, G. *J. Pept. Res.* **1997**, *50*, 451−457.
(36) Zouikri, M.; Vicherat, A.; Aubry, A.; Marraud, M.; Boussard, G. *J. Pept. Res.* **1998**, *52*, 19−26.
(37) Reynolds, C. H.; Horman, R. E. *J. Am. Chem. Soc.* **1996**, *118*, 9395−9401.
(38) Soth, M. J.; Nowick, J. S. *J. Org. Chem.* **1999**, *64*, 276−281.
(39) Donzel, B.; Rivier, J.; Goodman, M. *Biopolymers* **1974**, *13*, 2631−2647.
(40) Montagut, M.; Lemanceau, B.; Belloco, A.-M. *Biopolymers* **1974**, *13*, 2615−2629.
(41) Vicar, J.; Abillon, E.; Piriou, F.; Lintner, K.; Blaha, K.; Fromageot, P.; Fermandjian, S. *FEBS Lett.* **1979**, *97*, 275−278.
(42) Flurry, R. L., Jr.; Abdulnur, S. F.; Bopp, J. M., Jr. *Biopolymers* **1978**, *17*, 2679−2687.

to the stability of the *cis*-amide conformer for several TRH analogues[43] and suggested that the *cis*-amide conformer represents the receptor-bound conformation. A variety of approaches[12,44,45] to stabilizing the *cis*-amide conformer of the peptide bond have been proposed and reviewed.[46] A series of both *cis*- and *trans*-amide conformationally constrained analogues of TRH have been prepared,[47] and the consensus of the data favors the *trans*-amide-bond conformation as biologically relevant.[48,49]

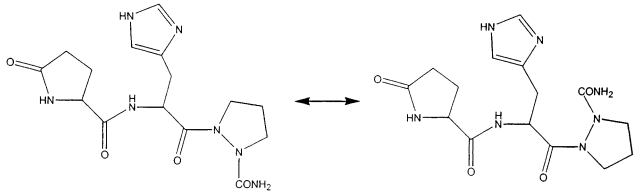

Methods

Conformational searches and molecular dynamics were performed with MacroModel[50] version 6.5. The MacroModel implementation of the AMBER all-atom force field was used for all of the calculations. The GB/SA continuum solvation model was used for the solution-phase calculations.[51] The calculations were done on a SGI Power Challenge L with 12 R10000 processors.

Conformational Searches. Conformational searches were performed by the systematic Monte Carlo Method of Goodman and Still.[52] For each search, 5000 starting structures were generated and minimized until the gradient was less then 0.05 (kJ/mol)/A^{-1}, using the truncated Newton−Raphson method implemented in MacroModel.[50] Duplicate conformations and those with energy greater than 50 kJ/mol above the global minimum found were discarded.

Monte Carlo/Stochastic Dynamics. All simulations were performed at 300 K with use of the Monte Carlo/Stochastic Dynamics (MC/SD) hybrid simulation algorithm[53] with the AMBER* force field as implemented in MacroModel 6.5.[50] A time step of 0.75 fs was used for the stochastic dynamics (SD) part of the algorithm. The MC simulation used random torsional rotations between ±60° and ±180° that were applied to all rotatable bonds except for the C−N amide bonds, of the azapeptide of interest, where the random rotation was between ±90° and ±180°. No rotations were applied to the bonds in the rings for proline and azaproline, as the transition barriers between ring conformers are low enough to permit adequate sampling from the SD part of the simulation. The total simulation was 2000 ps, and samples were taken at 1 ps intervals, yielding 2000 conformations for analysis.

Chemical Syntheses of [azPro^3]-TRH and [Phe^2, azPro^3]-TRH. To test the validity of the calculations in view of the experimental data from crystal structures and NMR in organic solvents suggesting a strong

Scheme 1. Synthesis of the Protected azPro-NH_2 Derivative and Its Use in the Preparation of [AzPro^3]-TRH[a]

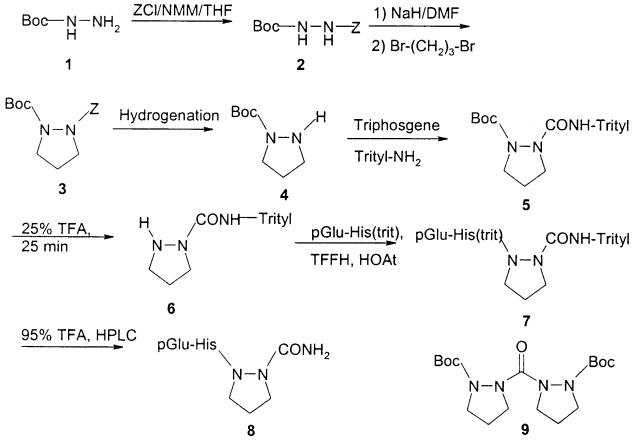

[a] An analogous procedure was used for the synthesis of [Phe^2, azPro^3]-TRH by reacting pGlu-Phe-OH with compound **6**.

stabilization of the *cis*-amide bond, [azPro^3]-TRH and [Phe^2, azPro^3]-TRH were synthesized by a novel synthetic route (Scheme 1) due to the relative lack of reactivity of azaproline. The synthesis of azapeptides was initially introduced by Goldschmidt and Wick[54] and actively developed by Gante[55,56] and by Dutta and Morley.[57] More recently, synthetic routes have been investigated by Gante,[56] Quibellet et al.,[58,59] and Gibson et al.[20] utilizing solid-phase synthesis, and also by Han et al.[31] using a liquid-phase approach. Incorporation of an aza-amino acid residue into the peptide chain requires a combination of hydrazine and peptide chemistry. The usual approach consists of adding a protected hydrazine to an isocyanate derivative of the peptide N-terminal, but it is not applicable when Pro occupies the N-terminal position. Another method uses activated aryl esters of aza residues, but the reaction needs high temperature and long reaction time, resulting in low yields with numerous side products, oxadiazolones, and hydantoins. Andre et al.[60] used triphosgene as the carbonylative reagent of a protected hydrazide. It is a mild, easy to handle, and efficient carbonylating agent for azapeptide synthesis. Alhough this method works well, in general, the activated species can only be prepared in situ (under N_2 at −10° C), and formation of considerable amounts of side products, such as diazatides, occurred.

Boc-hydrazine **1** was acylated by carbobenzoxychloride to afford Boc-NH-NH-Z **2**. Reaction with NaH in DMF and subsequent treatment by 1,3-dibromopropane afforded Boc-azPro-OBzl **3**. Removal of Z by hydrogenation gave Boc-*N*,*N*′-propylhydrazine **4**, which was activated with triphosgene below −10° C, and then reacted with tritylamine to give Boc-azPro-NH-Trt **5**. Removal of Boc with 25% TFA for 25 min gave azPro-NH-Trt **6**, which was reacted with the protected dipeptides, either pGlu-His(Trt)-OH or pGlu-Phe-OH after activation with TFFH/HOAT/DIEA, to obtain the protected tripeptides **7**. Next 95% TFA/CH_2Cl_2 was used to remove the trityl groups from both the carboxamide and the imidazole groups, and the crude TRH analogues **8** were purified by HPLC and characterized by ESI/MS (Scheme 1).

In this work, while making Boc-azPro-carbonyl chloride from **6** and triphosgene with NMM, the reaction of phosgene with **1** was incomplete, and starting material remained. When Boc-azPro-amide was prepared with anhydrous NH_3 in dioxane, side reactions occurred, and

(43) Liakopoulou-Kyriakides, M.; Galardy, R. E. *J. Med. Chem.* **1979**, *22*, 1952−1957.
(44) Zabrocki, J.; Smith, G. D.; Dunbar, J. B., Jr.; Iijima, H.; Marshall, G. R. *J. Am. Chem. Soc.* **1988**, *110*, 5875−5880.
(45) Paul, P. K. C.; Burney, P. A.; Campbell, M. M.; Osguthorpe, D. J. *Bioorg. Med. Chem. Lett.* **1992**, *2*, 141−144.
(46) Etzkorn, F. A.; Travins, J. M.; Hart, S. A. In *Advances in Peptidomimetics*; Abell, A., Ed.; JAI Press Inc.: Greenwich, CT, 1999; Vol. 2, pp 1−34.
(47) Tong, Y. S.; Olczak, J.; Zabrocki, J.; Gershengorn, M. C.; Marshall, G. R.; Moeller, K. D. *Tetrahedron* **2000**, *56*, 9791−9800.
(48) Laakkonen, L.; Li, W.; Perlman, J. H.; Guarnieri, F.; Osman, R.; Moeller, K. D.; Gershengorn, M. C. *Mol. Pharmacol.* **1996**, *49*, 1092−1096.
(49) Chu, W.; Perlman, J. H.; Gershengorn, M. C.; Moeller, K. D. *Bioorg. Med. Chem. Lett.* **1998**, *8*, 3093−3096.
(50) Mohamadi, F.; Richards, N. G. J.; Guida, W. C.; Liskamp, R.; Lipton, M.; Caufield, C.; Chang, G.; Hendrickson, T.; Still, W. C. *J. Comput. Chem.* **1990**, *11*, 440−467.
(51) Still, W. C.; Tempczyk, A.; Hawley, R. C.; Hendrickson, T. *J. Am. Chem. Soc.* **1990**, *112*, 6127−6129.
(52) Goodman, J. M.; Still, W. C. *J. Comput. Chem.* **1991**, *12*, 1110−1117.
(53) Guarnieri, F.; Still, W. C. *J. Comput. Chem.* **1994**, *15*, 1302−1310.
(54) Goldschmidt, S.; Wick, M. *Liebigs Ann. Chem.* **1952**, *575*, 217−231.
(55) Gante, J. *Chem. Ber.* **1965**, *98*, 540−547.
(56) Gante, J. *Synthesis* **1989**, 405−413.
(57) Dutta, A. S.; Morley, J. S. *J. Chem. Soc., Perkin Trans. 1* **1975**, 1712−1720.
(58) Gray, C. J.; Quibell, M.; Baggett, N.; Hammerle, T. *Int. J. Pept. Protein Res.* **1992**, *40*, 351−362.
(59) Quibell, M.; Turnell, W. G.; Johnson, T. *J. Chem. Soc., Perkin Trans. 1* **1993**, 2843−2849.
(60) Andre, F.; Marraud, M.; Tsouloufis, T.; Tzartos, S. J.; Boussard, G. *J. Pept. Sci.* **1997**, *3*, 429−441.

carbonyldi-*N*,*N*′(Boc)-propylhydrazine was formed. The probable reason is that NH_3 is a weaker base then **1**, so it did not compete with **1** to react with **2**. Instead of the desired reaction to produce the carboxamide, **1** left in solution due to the incomplete reaction with triphosphine reacted with **2** to form the undesirable symmetrical carbonyldihydrazide derivative **9**. When tritylamine, a stronger base than **1** or **2**, was used instead of NH_3, the tritylamine reacted smoothly with Boc-azPro-carbonyl chloride to give the desired product **5**.

Materials. $BocNHNH_2$, bis(trichloromethyl)carbonate, and tritylamine were purchased from Aldrich. His(Trt)-OMe was purchased from Bachem. Pyroglutamic acid (pGlu, pyrrolidone carboxylic acid) and trifluoroacetic acid (TFA) were purchased from Advanced Chemtech. HATu and HOAT were purchased from Richeliau Biotechnologies. Solvents were all HPLC grade. Tetramethylfluoroformamidinium hexafluorophosphate (TFFH)[61] was prepared in our laboratory. The purity of the peptides was confirmed by analytical HPLC (SP8800 Spectraphysics) with a C18 column (4.3 × 250 mm) and mass spectrometry. The mobile phase consisted of a gradient (B; 0.05% TFA in H_2O; B 0.038% TFA in 10% H_2O, 90% acetonitrile). The peptides were purified by HPLC chromatography using a Rainin Model HPX1, equipped with a Ranin C18 column (5μ 10 × 250 mm). The mobile phase consisted of the same two solvents as the analytical HPLC.

Procedure. 1. Boc-NHNH-Z. ZCl (0.1 M, 14.3 mL) was added dropwise to $Boc\text{-}NHNH_2$ (0.1 M, 13.2 g) in anhydrous THF (75 mL) containing NMM (0.1 M, 11 mL) at 0 °C. After being stirred for 12 h at room temperature, NMM·HCl salt was filtered off. THF was removed under reduced pressure to get an oil that was dried in desiccator overnight, when it became solid. The material was purified by flash chromatography with the solvent system, 7:3 = ethyl acetate:hexane, and was recrystallized with THF and hexane. Yield 85%, mp 63−64 °C, $R_f = 0.66$ (TLC solvent system, EtAc:hexane, 7:3). Mass: $M + 1 = 266$.

2. Boc-AzaPro Benzyl Ester. NaH (0.48 g, 0.02 M) in mineral oil (60% dispersion) was suspended in DMF (20 mL) under nitrogen at room temperature, and BocNHNHZ (0.01 M, 2.66 g) in DMF (10 mL) was added dropwise before the addition of 1,3-dibromopropane (0.01 M, 1.05 mL) in DMF (5 mL). When 1,3-dibromopropane was added, an ice-H_2O bath was used for the initial exothermic reaction, and the reaction solution was stirred under N_2 overnight. DMF was removed under reduced pressure, and the crude sample was taken up by AcOEt and washed successively with 0.1 M aqueous citric acid, 5% aqueous $NaHCO_3$, and brine. The crude sample obtained was purified by silica gel chromatography using the solvent system AcOEt:hexane = 7:3 as eluent; 4.43 mmol of pure sample was obtained. Yield = 44%, $R_f = 0.56$ (ETOAc:hexane = 7:3). Mass: $M + 1 = 306$.

3. Boc-azPro-tritylamide. Boc-azPro-benzylester (3 mmol, mw 305, 917 mg) was hydrogenated with Pd/C in methanol for 4 h. Pd/C was separated by filtration, and the solution was evaporated to dryness. Ether was added to the residue to give an oily solid (Boc-azPro-OH). NMM (mw = 101, $d = 0.92$, 3 mmol, 0.33 mL in THF 0.4 mL) was added dropwise under stirring to a cold solution (−10 °C) of triphosgene (mw = 296.75, 1 mmol, 297 mg) and BocAzapro (3 mmol in THF 3 mL) with stirring at −10 °C for 45 min. Tritylamine (mw 295.35, 3 mmol, 778.1 mg) and NMM (0.33 mL) were added progressively, and the solution was stirred overnight, followed by filtration and solvent evaporation. The residual oil was dissolved in EtOAc, and the solution was washed with 1 N $NaHCO_3$, 0.1 M citric acid, and brine. It was dried with Mg_2SO_4 and evaporated to dryness. The material was purified with the solvent system EtOAc:hexane = 4:6 on a silica gel column to yield a liquidlike oil that crystallized with EtAc and petroleum ether. Thus 260 mg of crystals (mw 456) was obtained. Yield = 60%, mp 132−133 °C. Mass: $M + 1 = 456$.

pGlu-His(Trt)-COOMe. Pyroglutamic acid (mw 129.2, 4 mmol, 1.792 g), HATu (mw 380.2, 4 mmol, 1.52 g), and HOAT (mw 136.1, 4 mmol, 544.4 g) were dissolved in DMF. DIEA (8 mmol, 1.392 mL) was added dropwise. His(Trt)-COOMe·HCl (4 mmol, mw 411.5, 1.6 g) was then added after being neutralized with 0.696 mL of DIEA. The pH was adjusted to 6.8, and the reaction was stirred overnight. The solvent was evaporated, and the residue was washed with 5% $NaHCO_3$, brine, ice-cold 0.1 N citric acid, and brine again to give an oily white solid. Mass: $M + 1 = 523$. Next 0.79 mmol of pGlu-His-(Trt)-COOMe (410 mg, mw 522.7) was dissolved in 0.79 mL of DMF. In an ice bath, 0.79 mL (1 N NaOH) was added dropwise to the solution with stirring. The extent of hydrolysis was checked by TLC (CHCl3: CH3OH:HOAc = 9:1:0.1) every 30 min, and the reaction was complete by 1 h and 40 min. Evaporating the DMF gave a white solid (214 mg, 53% yield). mp 132 °C, $R_f = 0.219$ in solvent system 9:1:0.1 ($CHCl_3$: methanol:HOAc). Mass: $M + 1 = 509$.

pGlu-His(Trt)-azPro-tritylamide. Boc-azPro tritylamide (182.4 mg, mw 456, 0.4 mM) was deprotected with 25% TFA/CH_2Cl_2 for 25 min to give TFA·azPro tritylamide. The mixture of TFFH (mw 266, 0.4 mM, 106.4 mg), HOAt (mw 136.1, 0.4 mM, 54.44 mg), and collidine (0.0525 mL in DMF 0.5 mL) was stirred at room temperature for 3 min and was added at 0 °C to 2 mL of DMF containing pGlu-His-(Trt)-COOH (203.48 mg, mw 508.7, 0.4 mM) and TFA. AzPro tritylamide (after being neutralized with collidine, 0.0525 mL) and then collidine 0.0571 mL were added; pH was 6. The trityl group was removed with 95% TFA for 1 h, and then the TFA was evaporated. After ethyl ether was added to the residue, a white precipitate developed that was filtered and dried.The crude sample was purified by reverse phase HPLC with the solvent system A: 0.05% TFA/H_2O; B: 0.038% TFA/90% acetonitrile and 10% H_2O; gradient 2-100% B 30′. The desired tripeptide, pGlu-His-azPro-NH_2, came out at 7.8 min (mw 363, 48 mg). Total yield = 35%, mp = 121 °C, $R_f = 0.836$ in 9:1:0.1 = $CHCl_3$:MeOH:HOAc). Mass: $M + 1 = 364$.

Biological Assay. The TRH analogues were tested for binding as well as signaling at the TRH receptor type 1, TRH-R1. Until recently, this was the only TRH receptor described, but a second receptor with a distinct distribution in the CNS has been described. Little to no differences were seen in binding or signaling between the two receptors for a set of TRH analogues.[62] Receptor binding of the TRH analogues was measured in TRH-R1 transfected COS-1 cells as previously described.[63] TRH-R1-mediated phosphoinositol hydrolysis was measured in *myo*-[^{3}H]inositol-labeled cells.[64] All analogues appear to be full agonists. The experimental values in the two assays as compared with control standards were as follows:

	EC_{50} (signaling) nM	IC_{50} (binding)
TRH	1.8 (0.77−4.4)	4.7 (2.4−9.3)
[Phe^2]-TRH	96 (66−150)	440 (140−1300)
[azPro^3]-TRH	74 (50−110)	860 (500−1400)
[Phe^2, azPro^3]-TRH	20 000 (7400−58 000)	>200 000

NMR Spectroscopy. NMR spectra were recorded with a Varian Unity-600 (Varian Assoc., Palo Alto, CA) spectrometer, and the data were processed off-line on a ULTRASPARC station with VNMR software. Proton and carbon chemical shifts were measured in parts per million (ppm) downfield from an external 3-(trimethylsilyl)propionic acid (TSP) standard. Proton spectra were obtained in 6100-Hz spectral width collected into 64K data points with 5.0 s pre-acquisition delay. Carbon spectra were obtained with a 32 000-Hz spectral width collected into 64k data points.

The total correlation (2D HOHAHA) spectra[65] were recorded using an MELV-17 mixing sequence of 100 ms, flanked by two 2 ms trim

(61) Carpino, L. A.; El-Faham, A. *J. Am. Chem. Soc.* **1995**, *117*, 5401−5402.
(62) O'Dowd, B. F.; Lee, D. K.; Huang, W.; Nguyen, T.; Cheng, R.; Liu, Y.; Wang, B.; Gershengorn, M. C.; George, S. R. *Mol. Endocrinol.* **2000**, *14*, 183−193.
(63) Colson, A. O.; Perlman, J. H.; Smolyar, A.; Gershengorn, M. C.; Osman, R. *Biophys. J.* **1998**, *74*, 1087−1100.
(64) Perlman, J. H.; Laakkonen, L. J.; Guarnieri, F.; Osman, R.; Gershengorn, M. C. *Biochemistry* **1996**, *35*, 7643−7650.
(65) Bax, A.; Davis, D. G. *J. Magn. Reson.* **1985**, *65*, 355.

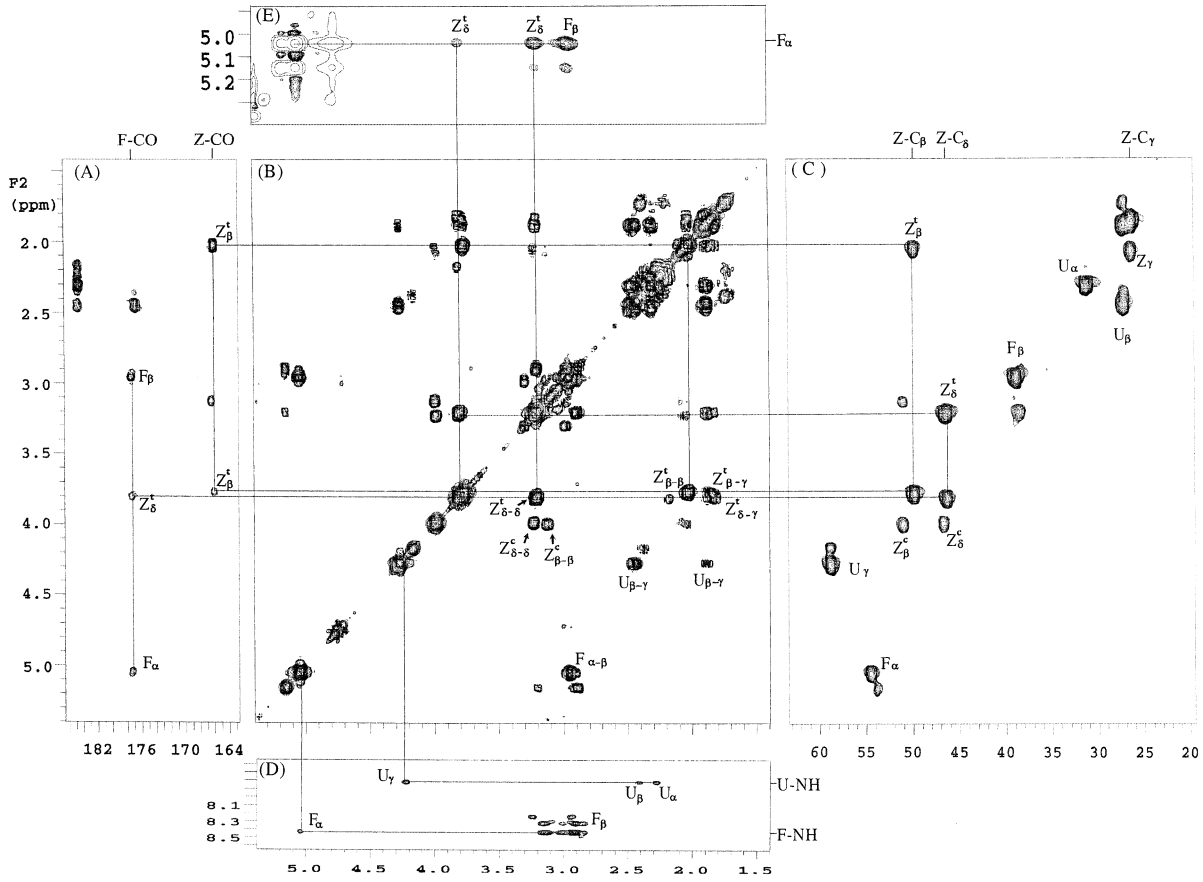

Figure 1. Expansions of the 600 MHz spectra of [Phe^2, azPro^3]-TRH in D_2O at 25 °C. (a) The HMBC spectrum in which the correlations of F−CO−F_α−F_β−Z_δ and Z−CO−Z_β are connected by lines. (b) The COSY spectrum shows the adjacent H^1−H^1 connectivity. (c) The HMQC spectrum shows the H^1−C^{13} connectivity. (d) The TOCSY spectrum shows the U and F amide NH to α, β, and γ correlations and (e) the NOE cross-peaks of Z_δ to F_α in *trans* F−Z amide conformation. The NOESY cross-peaks were distinguished from diagonal peaks by their negative character.

pulses. Phase-sensitive 2D spectra were obtained by employing the Hypercomplex method. A total of 2 × 256 × 2048 data matrix with 16 scans per t1 value were collected. Gaussian line broadening and a sine-bell function were used in weighting the t2 and t1 dimensions, respectively. After two-dimensional Fourier transform, the spectra resulted in 2048 × 2048 data points that were then phase- and baseline-corrected in both dimensions. A two-dimensional COSY[2] spectrum was collected into a 512 × 2048 data matrix with 16 scans per t1 value. The time-domain data were zero filled to yield a 2048 × 2048 data matrix and were Fourier transformed using a sine-bell weighting function in both t2 and t1 dimensions. The NOESY[3] spectrum resulted form a 2 × 256 × 2049 data matrix with 32 scans per t1 value. Specta were recorded with a 250 ms mixing time. The Hypercomplex method was used to yield phase-sensitive spectra. The time-domain data were zero filled to yield a 2k x 2k data matrix and were processed in a way similar to that of the 2D HOHAHA spectrum described above.

The proton-detected heteronuclear multiple quantum coherence (HMQC)[4] spectrum was recorded using a 0.35 s $^1H-^{13}C$ nulling period, and a 0.055 s delay was used in HMBC experiment. The 90° ^1H pulse width was 11 μs, and the 90° ^{13}C pulse width was 14 μs. The proton spectral width was set to 6100 Hz, and the carbon spectral width was set to 31 000 Hz. Phase-sensitive 2D spectra were obtained by employing the Hypercomplex method. A 2 × 256 × 2048 data matrix with 64 scans per t1 value was collected. Gaussian line broadening was used in weighting both the t2 and the t1 dimension. After two-dimensional Fourier transform, the spectra resulted in 512 × 2048 data points that were phase and baseline corrected in both dimensions.

Results and Discussion

NMR Studies. Proton and carbon chemical shifts of [azPro^3]-TRH and [Phe^2, azPro^3]-TRH (Scheme 1) were assigned by analysis of COSY, TOCSY, NOESY, HMQC, and HMBC spectra. Pyroglutamic acid (U) was identified first by the spin propagation from the amide NH through γ, β, and α protons (Figure 1d), and the U_γ proton was confirmed by the sequential $\gamma(i)$−NH (i + 1) connections between the adjacent U−H (His) or U−F (Phe) residues. Correlated proton resonances from NH at 8.45 ppm in Figure 1d were unambiguously assigned to F_α and F_β at 5.05 and 2.95 ppm, respectively. The assignments of azPro (Z) Z_δ and Z_β protons were made from the F (or H)−CO−Z_δ and Z−CO−Z_β HMBC correlations. Connections of F (or H)−CO−Z_β and Z−CO−Z_δ were ruled out due to the weak four-bond carbonyl carbon−proton couplings. F−CO resonance at 177.33 ppm (Figure 1a) was assigned on the basis of the unique F−CO to F_α, F_β, and Z_δ multiple-bond carbon−proton correlation. Likewise, the CO resonance at 174.52 ppm in Figure 2a was assigned to H−CO. Correlation from the carbonyl carbon at 166.14 ppm (Figure 1a) was assigned to Z−CO due to the connection to two Z_β protons only. Complete assignment of the azPro resonances in [azPro^3]-TRH was obtained by tracing the HMBC cross-peaks (Figures 1a and 2a) to cross-peaks of the same proton chemical shift at the COSY and HMQC spectra. Combined use of the adjacent H1−H1 connectivity in COSY and direct C13−H1 connectivity in HMQC allows for the

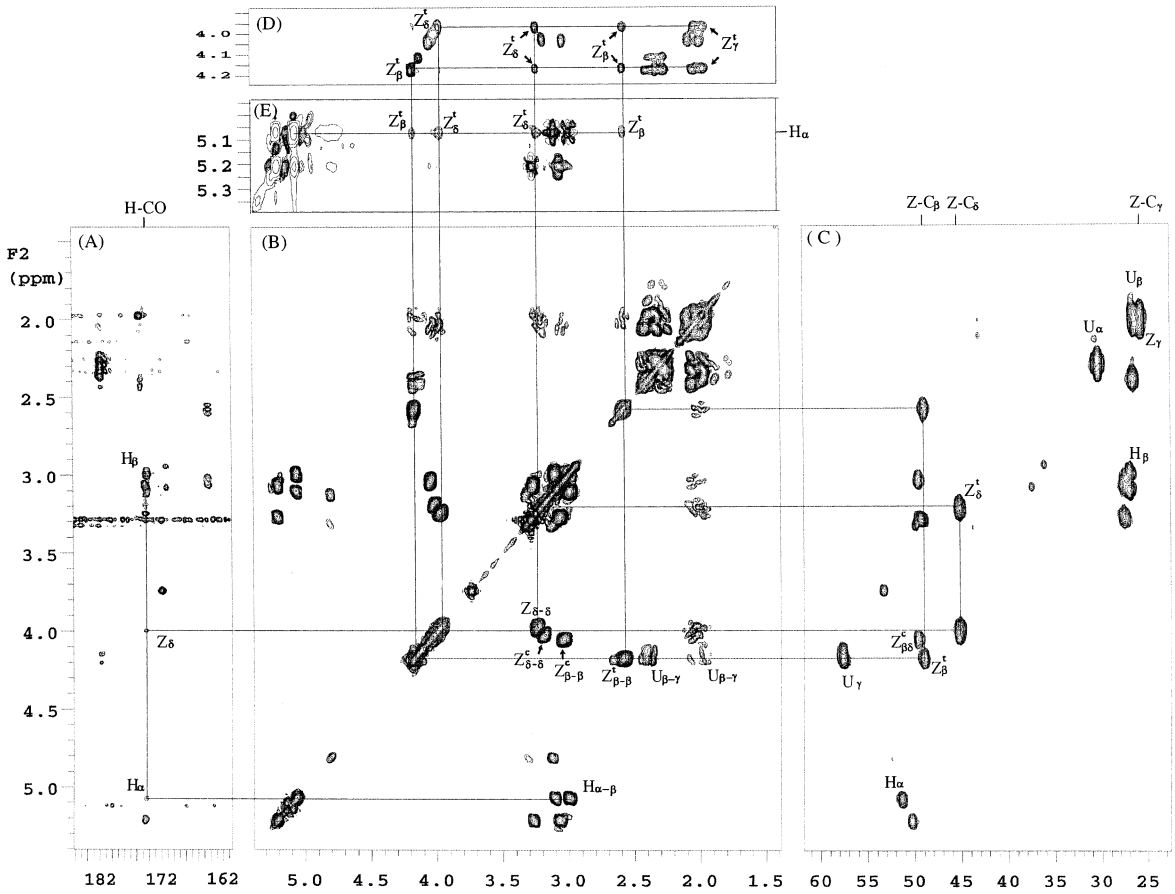

Figure 2. Expansions of the 600 MHz spectra of [azPro^3]-TRH in CD_3OD at −10 °C. (a) The HMBC spectrum in which the correlation of H−CO−H_α−H_β−Z_δ is connected by a line. (b) The COSY spectrum shows the adjacent H^1−H^1 connectivity. (c) The HMQC spectrum shows the H^1−C^{13} connectivity. (d) The TOCSY spectrum differentiates the Z_δ−Z_γ−Z_β spin propagation between *cis*- and *trans*-isomers of [azPro^3]-TRH, and (e) the NOE cross-peaks of Z_δ to H_α indicate the *trans* H−Z amide conformation.

removal of the ambiguity of assigning the geminal protons of the azaproline. For example, Z_δ resonance at 3.79 ppm (Figure 1b) shows two cross-peaks $Z_{\delta-\delta}$ and $Z_{\delta-\gamma}$ at 3.20 and 1.85 ppm. However, the HMQC reveals that both proton resonances at 3.79 and 3.20 ppm connect to the same carbon at 46.4 ppm (Z−C_δ) (Figure 1c), indicating that these are the Z_δ geminal protons. Resonance at 1.85 ppm (Figure 1b) was assigned to the Z_γ proton because it connects to a different carbon at 26.43 ppm (Z−C_γ) (Figure 1c). The same scheme was used for the assignment of the proton and carbon chemical shifts in [Phe^2, azPro^3]-TRH (Figure 2b and c).

The presence of azPro in the peptide produces *cis*- and *trans*-isomers of the F−Z and H−Z amide bond. This is reflected by the observation of two sets of cross-peaks for each individual H1 and C13 resonance, such as H_α, F_α, and U_γ in Figures 1c and 2c. To further differentiate the azaproline resonances between *cis*- and *trans*-isomers, use was made of the TOCSY spectra that correlate the spin propagation Z_δ−Z_γ−Z_β to the same isomer. Correlated peaks from resonances at 4.17 ppm (Z_β) and 3.98 ppm (Z_δ) showing in Figure 2d all belong to the same isomer, while spin propagation from 4.05 and 4.02 ppm in Figure 2d belongs to the other isomer. Furthermore, strong NOE cross-peaks between H_α (at 5.06 ppm) and Z_δ (at 3.98 and 3.23 ppm) (Figure 2e) were observed, indicating that the His-azPro amide bond appeared to be in the *trans*-conformation. Meanwhile, a weak correlation between H_α at 5.22 ppm and Z_δ at 4.02 ppm (Figure 2e) suggests these were the resonances of the *cis*-conformation. The same strategy was used to assign the *cis*- and *trans*-conformers of [Phe^2, azPro^3]-TRH (Figure 1e), and complete assignments of H^1 and C^{13} resonance for each residue of [azPro^3]-TRH and [Phe^2, azPro^3]-TRH are listed in Table 1.

Interestingly, it was found that the chemical shift differences for the two azPro β protons ($Z_\beta{}^t$) are quite large for both of the *trans*-amide conformers of [Phe^2, azPro^3]-TRH ($\Delta\delta$ = 1.75 ppm) and [azPro^3]-TRH ($\Delta\delta$ = 1.58 ppm). The large chemical-shift difference is rationalized by the more rigid azaproline ring that places one of the Z_β proton directly over the deshielding zone of the Z−CO carbonyl group and leads to the strong nonequivalence of the two β protons. The observed U_γ−F_{NH} (or H_{NH}) and F_α (or H_α)−Z_δ NOEs allowed one to identify [azPro^3]-TRH and [Phe^2, azPro^3]-TRH with the all *trans*-amide backbone conformation. However, the NOESY spectra of [azPro^3]-TRH (Figure 2e) showed that the H_α not only has NOE to Z_δ but also to Z_β protons, indicating that the H−Z amide bond deviates from a complete *trans*-amide conformation. Populations of the *cis*−*trans*-conformer estimate from the volume integral in HMQC and COSY spectra were approximately 40/60 for [azPro^3]-TRH and 20/80 for [Phe^2, azPro^3]-TRH.

Side-chain rotamer populations[5] of the Phe and His residues of *trans*-[azPro^3]-TRH and *trans*-[Phe^2, azPro^3]-TRH were calculated using the best fit for the values of the coupling constant $J_{\alpha H-\beta H}$. The $g-$ and t rotamer constituted the most dominate population (Table 1). The $g+$ rotamer is sterically

Table 1. Proton and Carbon Chemical Shifts (ppm) of [Phe^2, azPro^3]-TRH in D_2O at 25 °C and [azPro^3]-TRH in CD_3OD at −10 °C[a]

	NH	H_α	H_β	H_γ	H_δ	C_α	C_β	C_γ	C_δ	CO
Phe-aza										
U	7.83	2.33	2.44, 1.87	4.27		31.26	27.26	58.76		184.67 (CO1)
		(2.35)	(2.37, 1.72)	(4.15)		(30.32)	(27.23)	(58.85)		176.80 (CO2)
F	8.45	5.05	2.95			54.56	38.79			177.33
		(5.15)	(3.19, 2.94)			(53.89)	(38.59)			
			$J_{\alpha\beta} = 7.8$[c]							
			$g-$, $t \approx 48\%$							
Z			3.77, 2.02	2.03, 1.85	3.79, 3.20		49.92	26.43	46.40	166.04
			(3.99, 3.13)		(3.99, 3.22)		(51.08)		(46.72)	
His-aza										
U	7.87[b]	2.28	2.39, 1.97	4.18		30.40	26.54	57.68		181.66 (CO1)
				(4.13)				(57.59)		175.18 (CO2)
H	8.65[b]	5.06	3.01, 3.00			51.42	26.96			174.52
		(5.22)	(3.26, 3.07)			(50.30)	(27.53)			
			$J_{\alpha\beta} = 5.8, 8.9$[c]							
			$g- \approx 58\%$, $t \approx 29\%$							
Z			4.17, 2.59	2.03	3.98, 3.23		49.03	25.84	45.19	164.38
			(4.05, 3.04)		(4.02, 3.18)		(49.57)		(49.32)	

[a] Chemical shifts of *cis*-amide conformers are shown in parentheses. [b] In 90% H_2O at 25 °C. [c] *J* coupling constant in Hz with rotamer population $g-$ and *t* in percentage.

unfavored due to interaction between the F, H aromatic groups and the azaproline ring. The *t* rotamer may constitute up to 50% of the population in [azPro^3]-TRH that places the His aromatic ring in the region near the Z_δ protons. Ring-current effects from the His imidazole may contribute more significantly to the nonequivalence of two Z_δ protons in [azPro^3]-TRH ($\Delta\delta = 0.75$ ppm) than does Zδ in [Phe^2, azPro^3]-TRH ($\Delta\delta = 0.59$ ppm).

Calculations. In earlier versions of MacroModel, no parameters were available for aza-amino acids, so the proper parameters for the AMBER* force field were estimated with ab initio calculations. With the release of MacroModel 6.5, this effort became redundant because this version included parameters for aza-amino acids in agreement with those estimated. By focusing on azaproline, we minimized the impact of the parameters for the central N−N bond because the torsional rotation of this bond is relatively fixed for the azPro ring.

Conformational Searches. Monte Carlo searches were performed on the blocked aza-containing tetrapeptides Ac-Ala-Xxx-Yyy-Ala-NHMe, the blocked aza-tripeptides Boc-Ala-Xxx-Ala-NHiPr, and on the TRH tripeptides. The calculations included the GB/SA solvation model and the AMBER* force field parameters as implemented in MacroModel version 6.5. As reported by Boussard et al.,[34,35] the nitrogens in azaproline, especially the α-nitrogen, are not planar due their sp^3 character. The reported out-of-plane distance for the nitrogen is between 0.18 and 0.40 Å. This perturbation results in both nitrogens being prochiral; they can either be *S,S* or *R,R*. Both diastereomers have been studied to compare the influence of the conformation on the reverse-turn propensity. The energy differences between the *cis*- and *trans*-conformations are calculated between the conformations with the lowest energy independent of whether it is (*R,R*) or (*S,S*). Hence, we assumed that the atoms attached to the nitrogens in the azPro ring can invert from *R* to *S* and vice versa.

TRH. The results from the conformational searches (see Table 2) show that the *trans*-conformation is more stable than the *cis*-conformation for TRH. The same is seen for TRH with azaproline in the C-terminal position; the *trans*-conformation is more stable than the *cis*-conformation. Comparing the *cis*- and *trans*-conformations reveals that the *trans*-conformation may be stabilized in these two compounds by an internal hydrogen bond. Changing the imidazole ([azPro^3]-TRH) ring to a phenyl ring ([Phe^2, azPro^3]-TRH) removed the possibility of an internal hydrogen bond. This makes the *cis*-conformation more stable, as can be seen in the Table 2.

Table 2. Results from the Conformational Searches To Determine the Relative Stability of *cis*−*trans*-Conformers[a]

	ω2		
peptide	cis kJ/mol	trans kJ/mol	ΔE (cis − trans) kJ/mol
Ac-Ala-Pro-azPro(*R,R*)-Ala-NHMe	−277.0	*−283.5*	−4.6
Ac-Ala-Pro-azPro(*S,S*)-Ala-NHMe	**−288.1**	−265.4	
Ac-Ala-azPro(*R,R*)-Pro-Ala-NHMe	277.4	−278.0	−0.5
Ac-Ala-azPro(*S,S*)-Pro-Ala-NHMe	**−284.2**	*−283.7*	
Ac-Ala-Ala-azPro(*R,R*)-Ala-NHMe	−398.8	*−399.8*	−4.2
Ac-Ala-Ala-azPro(*S,S*)-Ala-NHMe	**−404.0**	−396.0	
Boc-Ala-azPro(*R,R*)-Ala-NHiPr	−290.0	*−292.8*	−3.5
Boc-Ala-azPro(*S,S*)-Ala-NHiPr	**−296.3**	−288.8	
Boc-Ala-azPro(*R,R*)-Ala-NHiPr ($CHCl_3$)	−311.2	−306.9	−7.9
Boc-Ala-azPro(*S,S*)-Ala-NHiPr ($CHCl_3$)	**−315.8**	*−307.9*	
Boc-Ala-azPro(*R,R*)-D-Ala-NHiPr	−290.1	−296.0	−2.2
Boc-Ala-azPro(*S,S*)-D-Ala-NHiPr	**−298.2**	*−286.1*	
TRH	−363.1	***−367.6***	4.5
[azPro(*R,R*)^3]-TRH	−338.3	−336.4	2.4
[azPro(*S,S*)^3]-TRH	−338.4	***−340.9***	
pGlu-Phe-Pro-NH_2	**−306.5**	*−306.3*	−0.3
pGlu-Phe-azPro(*R,R*)-NH_2	−278.8	*−284.3*	−1.2
pGlu-Phe-azPro(*S,S*)-NH_2	**−285.5**	−279.6	

[a] The minimum found for each set of four diastereomeric (*RR, SS*) azPro *cis*−*trans*-conformers is indicated in bold. In the peptides not containing azPro, the minimum found for the *cis*−*trans*-conformer pairs is indicated in bold. The Δ*E* column denotes the difference between the lowest energy conformer (bold) and the lower of the other *cis*−*trans*-amide column for the peptide.

The conformational preference of these TRH analogues was examined by NMR in water and in methanol. In methanol at −10°, the signals from the *cis*- and *trans*-conformers of [azPro^3]-TRH were resolved and could be clearly assigned. The ratio of *cis*−*trans*-conformers estimated from the volume integrals in the HMQC and COSY spectra is approximately 40/60 for [azPro^3]-TRH and 20/80 for [Phe^2, azPro^3]-TRH. Comparing the *cis*- and *trans*-conformations reveals that the *trans*-conformation of [azPro^3]-TRH is stabilized by an internal

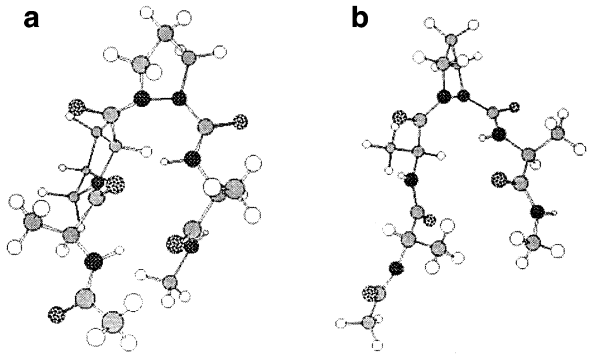

Figure 3. Structures of the global energy minimum found by a Monte Carlo using the AMBER* force field and the GB/SA solvation model. (a) Ac-Ala-Ala-AzPro(*S,S*)-Ala-NHMe. (b) Ac-Ala-Pro-AzPro(*S,S*)-Ala-NHMe.

hydrogen bond between its His[2] imidazole ring and a backbone amide bond. Changing the imidazole (His[2]) ring to a phenyl ring (Phe[2]) removes the possibility of this internal hydrogen bond. Thus, while the exchange of the carbon-α by nitrogen enhances the propensity for the *cis*-conformer, the conformational preference of azPro is obviously environmentally sensitive as seen both experimentally and computationally. The strength of this constraint is, therefore, insufficiently strong to hold the amide predominately in the *cis*-conformer regardless of the environment. Other constraints such as the 1,5-tetrazole amide-bond surrogate[66] or other bicyclic analogues[47] may be more appropriate to probe recognition of the *cis*-amide bond conformer by the receptor.

The affinity of [azPro[3]]-TRH for the TRH receptor from the anterior pituitary was reduced 40-fold as compared to that for TRH itself, consistent with significantly reduced activity seen in general for analogues with *cis*-amide constraints.[47] [Phe[2]]-TRH has a lower affinity for the TRH receptor than TRH itself, and the substitution of azPro for Pro in the [Phe[2], azPro[3]]-TRH analogue causes an approximately 200-fold further loss in affinity.

Tetrapeptides. The results from the conformational search are shown in Table 2. It can be seen that the *S,S*-conformer is the most stable for the *cis*-conformation, in agreement with Boussard et al.[34] The same thing is not observed for the *trans*-conformations; the (*S,S*) does not seem to be favored over the (*R,R*) diastereomers. For the Ac-Ala-Pro-azPro(*S,S*)-Ala-NHMe peptide, the *cis*-conformation is the most stable one, 4.6 kJ/mol more stable than the *trans*-conformation. The minimum energy conformation of Ac-Ala-Pro-azPro(*S,S*)-Ala-NHMe is shown in Figure 3a. It is clear from the figure that the structure forms a type VIa β-turn with a *cis*-conformation for the preceding azPro residue ($\omega_2 = 19.0°$) and with $\Phi_2 = -37.4°$, $\Psi_2 = 122.6°$, $\Phi_3 = -92.5°$, and $\Psi_3 = 14.8°$. The conformation in Figure 3a is stabilized with an internal hydrogen bond between the carbonyl oxygen at residue one and the amide hydrogen of residue four. There is also a second hydrogen bond between the two end groups.

Moving the azaproline to the second residue only gave a small difference between the lowest energy conformations with a *cis*- versus a *trans*-amide bond; the difference was only 0.5 kJ/mol. This is in accordance with what Boussard et al.[34] found, that the amide bond preceding the azPro is favored, and not the one after the azPro.

Changing the second residue to an alanine, Ac-Ala-Ala-azPro-Ala-NHMe, which is more flexible than proline, does not change the energy difference between *cis*- and *trans*-conformers much, but the minimum is a type VIb β-turn instead of a type VIa β-turn. The lowest energy conformation for Ac-Ala-Ala-azPro-(*S,S*)-Ala-NHMe is shown in Figure 3b with the following torsional angles: $\omega_2 = 11.7°$, $\Phi_2 = -159.3°$, $\Psi_2 = 138.4°$, $\Phi_3 = -91.0°$, and $\Psi_3 = 13.9°$. The reverse turn is not stabilized with any internal hydrogen bonds, also in good agreement with what has been found in other examples of type VIa β-turns.[1] Also, the differences between the *S,S*- and the *R,R*-configurations are less, indicating that these peptides are more flexible than the one with two pralines, as expected.

For comparison, we also included two tripeptides appearing in the paper by Boussard et al.[67] studied both in the crystalline state and, more recently, in chloroform solution by NMR. The two tripeptides are Boc-Ala-azPro-Ala-NHiPr and Boc-Ala-azPro-Ala-NHiPr, both reported to induce a β-turn in the sequence. Both show similar behavior according to the calculations; both favor the *S,S*-diasteriomer and the *cis*-conformation. This was also seen in the published NMR studies; however, there was no evidence for cis−trans equilibrium for the ω1− amide bond. It is important to remember that the NMR studies were not done in water, but in $CHCl_3$. The corresponding results with the $CHCl_3$ GB/SA solvation model are also shown in Table 2. The most stable conformation by simulation under similar conditions is also the *S,S*-diasteriomer with the *cis*-amide conformation.

Monte Carlo/Stochastic Dynamics. The results from the MC/SD runs are less conclusive than the results from the conformational searches. The differences between the *R,R*- and the *S,S*-diastereomers are quite large for [azPro[3]]-TRH and, especially, for [Phe[2], azPro[3]]-TRH.

The same set of geometrical parameters for characterizing the reverse turn was used as those previously by Takeuchi et al.[10] in a similar study on reverse-turn induction in tetrapeptides. We also included the number of conformations from the MD/SD simulation that have a *cis*-conformation for the central amide bond, because this is required for a type VI β-turn. The virtual torsion, β, defined by Cα1, Cα2, Cα3, and N4,[68,69] gives a measurement on the tightness of the turn. A torsion angle less than ±30° indicates a turn. The third parameter is that the Cα1−Cα4 distance must be less than 7 Å. The fourth and fifth parameters are the distance between the carbonyl at position one and the amide hydrogen of residue four with the cutoff distances set at 4 and 2.5 Å, respectively; within 4 Å indicates an interaction between these groups,[70] and within 2.5 Å indicates a hydrogen bond.[9] A slightly modified definition was used for the tripeptides because these only have three residues, but the results are still comparable. Also, in these calculations, both of the diastereomers were considered to account for the inversion of the nitrogens in the azPro ring that occurs, but is hard to simulate quantita-

(66) Zabrocki, J.; Marshall, G. R. In *Peptidomimetics Protocols*; Kazmierski, W. M., Ed.; Humana Press: Totowa, NJ, 1998; Vol. 23, Chapter 424, pp 417−436.
(67) Boussard, G.; Marraud, M. *J. Am. Chem. Soc.* **1985**, *107*, 1825−1828.
(68) Ball, J. B.; Andrews, P. R.; Alewood, P. F.; Hughes, R. A. *FEBS Lett.* **1990**, *273*, 15−18.
(69) Ball, J. B.; Hughes, R. A.; Alewood, P. F.; Andrews, P. R. *Tetrahedron* **1993**, *49*, 3467−3478.
(70) Constantine, K. L.; Mueller, L.; Andersen, N. H.; Tong, H.; Wandier, C. F.; Friedrichs, M. S.; Bruccoleri, R. E. *J. Am. Chem. Soc.* **1995**, *117*, 10841−10854.

Table 3. Results from the 1000 ps, 300 K MC/SD Run Using the GB/SA Solvation Model and the AMBER* Force Field in MacroModel 6.5

				%*d* (C═O···H–N)	
peptide	%ω2 cis	%$\lvert\beta\rvert$ < 30°	%*d* < 7 Å	<4 Å	<2.5 Å
Ac-Ala-Pro-Pro-Ala-NHMe	28.9	23.9	28.8	27.5	3.5
Ac-Ala-Pro-AzPro(*R*,*R*)-Ala-NHMe	61.9	35.4	38.2	36.1	19.5
Ac-Ala-Pro-AzPro(*S*,*S*)-Ala-NHMe	54.7	26.2	53.4	53.8	39.4
Ac-Ala-AzPro(*R*,*R*)-Pro-Ala-NHMe	36.5	7.5	28.0	19.3	0.2
Ac-Ala-AzPro(*S*,*S*)-Pro-Ala-NHMe	11.1	10.5	13.9	12.0	1.3
Ac-Ala-Ala-AzPro(*R*,*R*)-Ala-NHMe	37.9	52.4	32.9	0.9	0.2
Ac-Ala-Ala-AzPro(*S*,*S*)-Ala-NHMe	77.8	67.3	66.8	16.1	0.0
Ac-Ala-AzPro(*R*,*R*)-Ala-Ala-NHMe	0.0	6.1	15.5	0.0	0.0
Ac-Ala-AzPro(*S*,*S*)-Ala-Ala-NHMe	61.3	56.7	66.1	1.2	0.1
Boc-Ala-AzPro(*R*,*R*)-Ala-NHiPr	51.6	39.4	34.7	6.9	1.4
Boc-Ala-AzPro(*S*,*S*)-Ala-NHiPr	72.7	62.1	68.2	20.8	3.5
Boc-Ala-AzPro(*R*,*R*)-D-Ala-NHiPr	98.6	50.8	44.6	8.4	1.1
Boc-Ala-AzPro(*S*,*S*)-D-Ala-NHiPr	99.0	71.5	77.1	21.5	1.8
TRH	35.7				
AzTRH(*R*,*R*)	51.1				
AzTRH(*S*,*S*)	34.7				
pGlu-Phe-ProNH2	63.8				
pGlu-Phe-Pro(*R*,*R*)NH2	33.4				
pGlu-Phe-Pro(*S*,*S*)NH2	78.0				

tively without extensive parametrization. For TRH and [azPro^3]-TRH, only the percentage of *cis*-amide bond was used as a descriptor, because other parameters were not easily measured.

A summary of the MC/SD runs is shown in Table 3. To compare the conformational space for the different peptides, a plot of the backbone torsional angle Φ against angle Ψ for residue two and three was also used with other similar plots.

TRH and [azPro^3]-TRH. The results from the MC/SD simulation on both TRH and [azPro^3]-TRH are given in Table 2. Both of the tripeptides have a similar number of conformations with a *cis*-amide bond, 35.7% for TRH, 34.7% for [azPro^3]-TRH (*S*,*S*), and a slightly higher 51.1% for [azPro^3]-TRH (*R*,*R*). The Φ and Ψ plots for the His^2 and Pro^3 residues are shown in Figure 4a,b for TRH, and in Figure 4c,d for [azPro^3]-TRH. The conformational spaces are similar for the two tripeptides; the His^2 residue is restricted for both TRH and [azPro^3]-TRH. A similar trend is seen for the Pro^3 and azPro^3 residues. Changing the His^2 to a Phe increases the number of conformations with a *cis*-amide bond in the MD/SD simulation, as seen in Table 2. Only the [azPro^3]-TRH (*R*,*R*) diastereomer shows a lower degree of *cis*-amide bond. The conformational space is still restricted, and the Φ and Ψ angles for pGlu-Phe-Pro(*S*,*S*)NH_2 are shown in Figure 4 e,f; there are no large differences as compared to the Φ and Ψ plot for [azPro^3]-TRH.

Ac-Ala-Pro-Pro-Ala-NHMe. As a "reference" peptide, the Ac-Ala-Pro-Pro-Ala-NHMe tetrapeptide was included to enable comparison of this unmodified peptide with other analogues to determine the impact of modifications. Table 2 shows that 28.9% of the conformations from the MD/SD simulation have a *cis*-amide bond between the two central prolines. This indicates that the energy difference between the *cis*- and the *trans*-conformation of the intervening amide bond is not large. Also notable, only 3.5% of the conformations form a strong hydrogen bond between the carbonyl oxygen at residue one and the amide hydrogen at residue four, and 28.8% have a Cα1−Cα4 distance of less than 7 Å. The plot of torsional angles Φ_2 versus Ψ_2 and Φ_3 versus Ψ_3 is shown in Figure 5a,b. The torsional space for the second residue is restricted, as seen in Figure 5a. The conformation is also independent of the conformation for the amide bond because both the squares and the diamonds are mixed in the plot. The third residue is less constrained as the Φ_3 versus Ψ_3 plot shows in Figure 5b. The angle Ψ_3 is less well defined, ranging from about −70° to 180°. The *cis*-conformation for the central amide bond is a requirement for a hydrogen bond between the carbonyl oxygen and the amide hydrogen, and this can be seen in Figure 5c, the distance between the carbonyl oxygen and the amide hydrogen versus the amide torsion (ω_2). The Pro-Pro peptide forms a type VI β-turn, but it is not the dominant conformation in the MD/SD simulation, as can be seen in Table 3.

Ac-Ala-Pro-azPro(*S*,*S*)-Ala-NHMe and Ac-Ala-Pro-azPro-(*S*,*S*)-Ala-NHMe. As seen in Table 2, 54.7% of the samples in the simulations Ac-Ala-Pro-azPro(*S*,*S*)-Ala-NHMe have a *cis*-conformation for the central amide bond; for example, it likely forms a type VI β-turn. The same value for the *R*,*R* diastereomer is 61.9%. The Ψ_2 versus Φ_2 and Ψ_3 versus Φ_3 plot for Ac-Ala-Pro-azPro(*S*,*S*)-Ala-NHMe shows that the $\Phi\Psi$ space is well defined for both residues two and three, Figure 6a,b. The torsion angles seem to be independent of the ω2 torsion because the diamonds (cis) and squares (trans) are mixed in both of the plots. For the *cis*-conformations, all conformations have the type VIa β-turn with mean torsion angles, for all conformations with a *cis*-bond, of $\omega_2 = 16.5°$, $\Phi_2 = -53.2°$, $\Psi_2 = 135.2°$, $\Phi_3 = -94.6°$, and $\Psi_3 = 11.5°$. The population in the simulations that had a virtual torsion of $|\beta| < 30°$ was 26.2% for the *S*,*S* conformation; Figure 6c shows the distance between the carbonyl oxygen of residue one and the amide hydrogen of residue four. It is clear that those conformations with a central *cis*-amide bond (diamonds) have a virtual torsion angle around 30° (mean virtual torsion angle for the *cis*-conformations is 30.8°). 39.4% of the conformations in the simulations have a strong hydrogen bond with a length less than 2.5 Å, a significantly high value. This indicates that only conformations with a *cis*-amide bond are able to form a reverse turn for this peptide. Figure 6d, the hydrogen bond distance versus ω2, clearly indicates that this is the case; the only allowed β-turn is the type VIa β-turn. The number of structures from the MD/SD simulation with a Cα1−Cα4 distance less than 4 Å is 53.4%.

The results for the *R*,*R* diastereomer differ in several ways. As seen in Figure 6e, the hydrogen bonds are only possible for

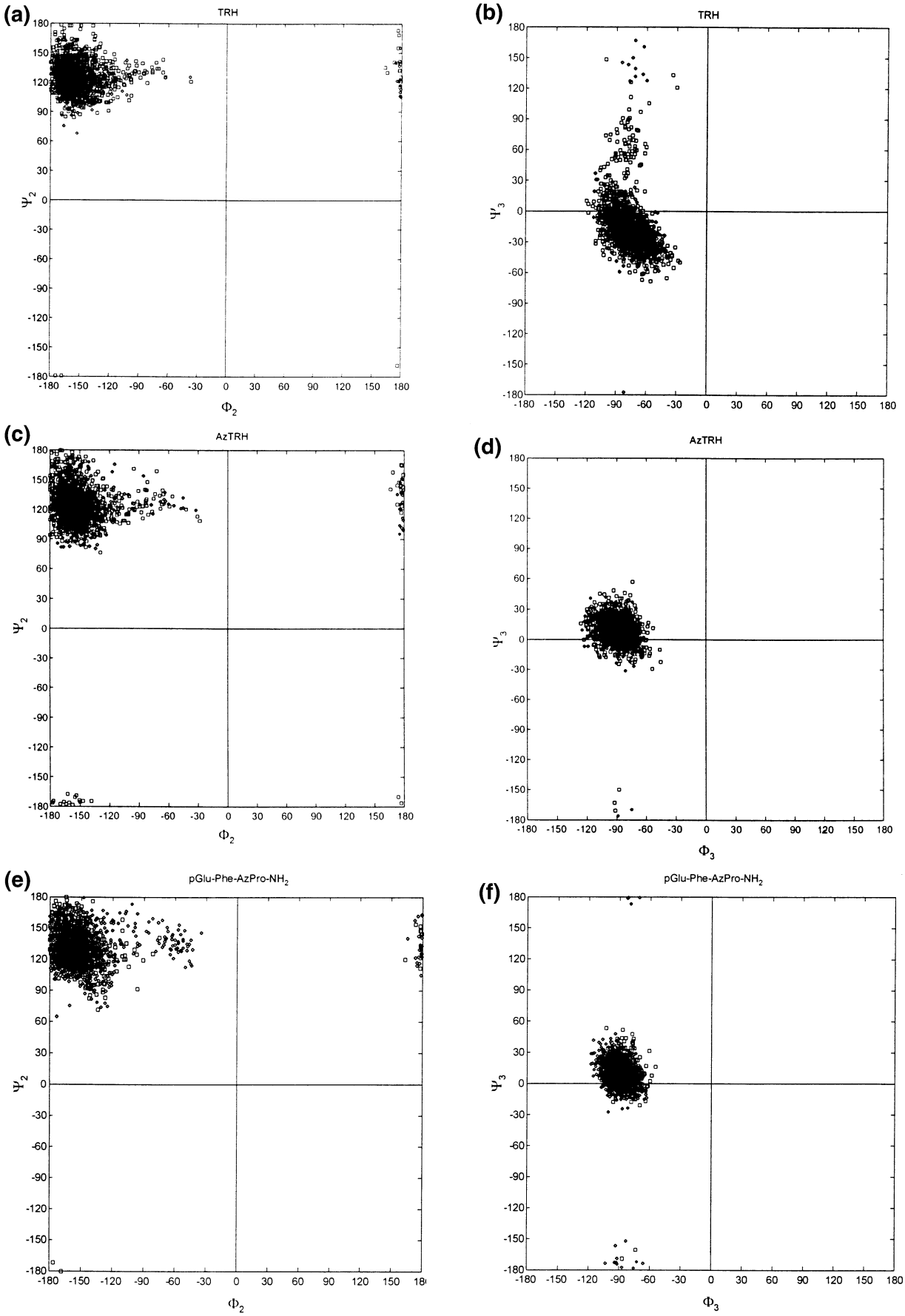

Figure 4. Results from the MC/SD simulations. ◇ − Structures with a *cis*-amide bond; ◆ − structures with a *trans*-amide bond. (a) Ψ_2 vs Φ_2 for TRH. (b) Ψ_3 vs Φ_3 for TRH. (c) Ψ_2 vs Φ_2 for [azPro^3]-TRH. (d) Ψ_3 vs Φ_3 for [azPro^3]-TRH. (e) Ψ_2 vs Φ_2 pGlu-Phe-azPro(*S*,*S*)NH_2. (f) Ψ_3 vs Φ_3 for pGlu-Phe-azPro(*S*,*S*)NH_2.

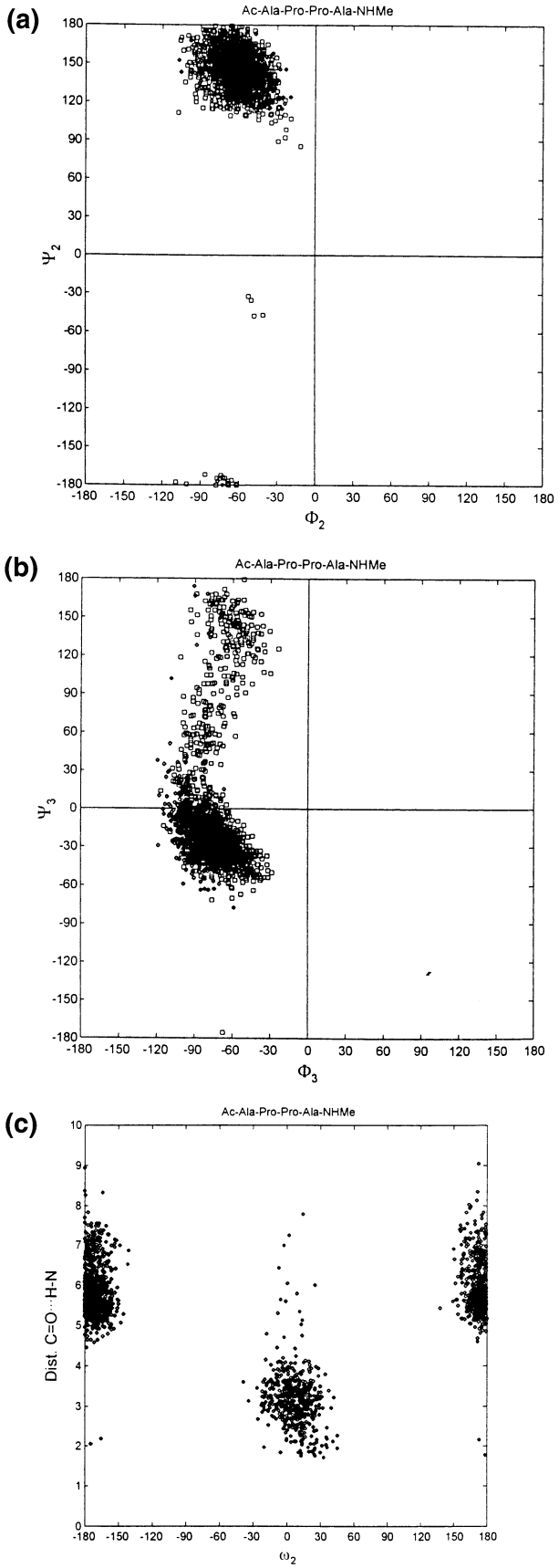

Figure 5. Results from the MC/SD simulations for Ac-Ala-Pro-Pro-Ala-NHMe. ◇ − Structures with a *cis*-amide bond; ◆ − structures with a *trans*-amide bond. (a) Ψ_2 vs Φ_2 for Ac-Ala-Pro-Pro-Ala-NHMe. (b) Ψ_3 vs Φ_3 for Ac-Ala-Pro-Pro-Ala-NHMe. (c) Hydrogen bond distance vs ω_2 for Ac-Ala-Pro-Pro-Ala-NHMe.

the *trans*-conformations; 19.5% of the population has a hydrogen bond length less than 2.5 Å. The reverse turn is also tighter as can be seen from Figure 6f, comparing the hydrogen bond distance versus the virtual torsion β. The mean value for the virtual torsion angle is 6.5° for the conformation with a *trans*-amide bond (squares). The mean Φ and Ψ torsion angles for the second and third residue are $\Phi_2 = -58.2°$, $\Psi_2 = 131.2°$, $\Phi_3 = 83.5°$, and $\Psi_3 = -8.9°$. Both of the two diastereomers show a high degree of reverse turn, even if the *R,R* diastereomer requires a *trans*-amide bond, while the *S,S* diastereomer requires a *cis*-amide bond, that is, a type VIa β-turn.

Ac-Ala-azPro(*S,S*)-Pro-Ala-NHMe and Ac-Ala-azPro-(*R,R*)-Pro-Ala-NHMe. Few of the sampled conformations of these peptides form a tight turn; only 7.5% and 10.5% for the *R,R* and *S,S*, respectively, have a virtual torsion less than 30°. Table 2 shows that few of the sampled conformations form a strong hydrogen bond between the carbonyl oxygen at residue one and the amide hydrogen at residue four. The *R,R* diastereomer has some interactions between the carbonyl oxygen and the amide hydrogen: 19.3% of the samples have a distance less than 4 Å, but only 0.2% less than 2.5 Å, indicating few strong hydrogen bonds. The degree of reverse turn is even less than that for the tetrapeptide with two ordinary residues at residue two and three. An azPro (*SS* or *RR*) at residue two decreases the likelihood for a *cis*-amide bond at its C-terminal, and, therefore, it is also a type VI β-turn for the tetrapeptide.

Ac-Ala-Ala-azPro(*R,R*)-Ala-NHMe and Ac-Ala-Ala-az-Pro(*S,S*)-Ala-NHMe. The Ac-Ala-Ala-azPro-Ala-NHMe tetrapeptides are less restricted as compared to the tetrapeptides with two central proline residues. As seen in Table 3, a higher degree of the conformations in the MD/SD simulation has the *cis*-conformation; for the *S,S* diastereomer, the value is 77.8%. The *S,S* diastereomer also shows a high degree of β-turn according to the virtual torsion angle and the Cα1−Cα4 distance, 67.3 and 66.8%, respectively. The Φ and Ψ plots for residues two and three are shown in Figure 7a,b. There is no difference in Φ and Ψ space between conformations with a *cis*-amide bond (diamonds) or conformations with a *trans*-amide bond (squares). The mean Φ2 angle for conformations with a *cis*-amide bond is shifted −100° degrees as compared to that of the Ac-Ala-Pro-azPro(*S,S*)-Ala-NHMe peptide. The mean value for the torsional angles are $\omega_2 = 11.0°$, $\Phi_2 = -149.0°$, $\Psi_2 = 138.7°$, $\Phi_3 = -91.6°$, and $\Psi_3 = 8.43°$. This is closer to the type VIb β-turn instead of the VIa β-turn for the Ac-Ala-Pro-azPro(*S,S*)-Ala-NHMe peptide. From Figure 7c, ω_2 versus hydrogen bond distance, it is clear that the *cis*-conformation gives the shortest distances between the carbonyl oxygen and the amide hydrogen. The distance is still too long for making good hydrogen bonds. We can also see from Figure 7d, virtual torsion angle versus hydrogen bond distance, that all of the conformations with a *cis*-amide bond (diamonds) have a virtual torsion angle around zero (mean virtual torsion for the *cis*-conformations is 7.0°). This indicates that the peptide makes a tight reverse turn, but there is no internal hydrogen bonding involved. The *R,R* diastereomer showed less propensity for reverse-turn formation as seen in Table 1. All of the conformations from the MD/SD simulation that showed a reverse turn had a *trans*-conformation for the middle amide bond, similar for the *R,R* diasteriomer of the Ac-Ala-Pro-azPro-Ala-NHMe peptide.

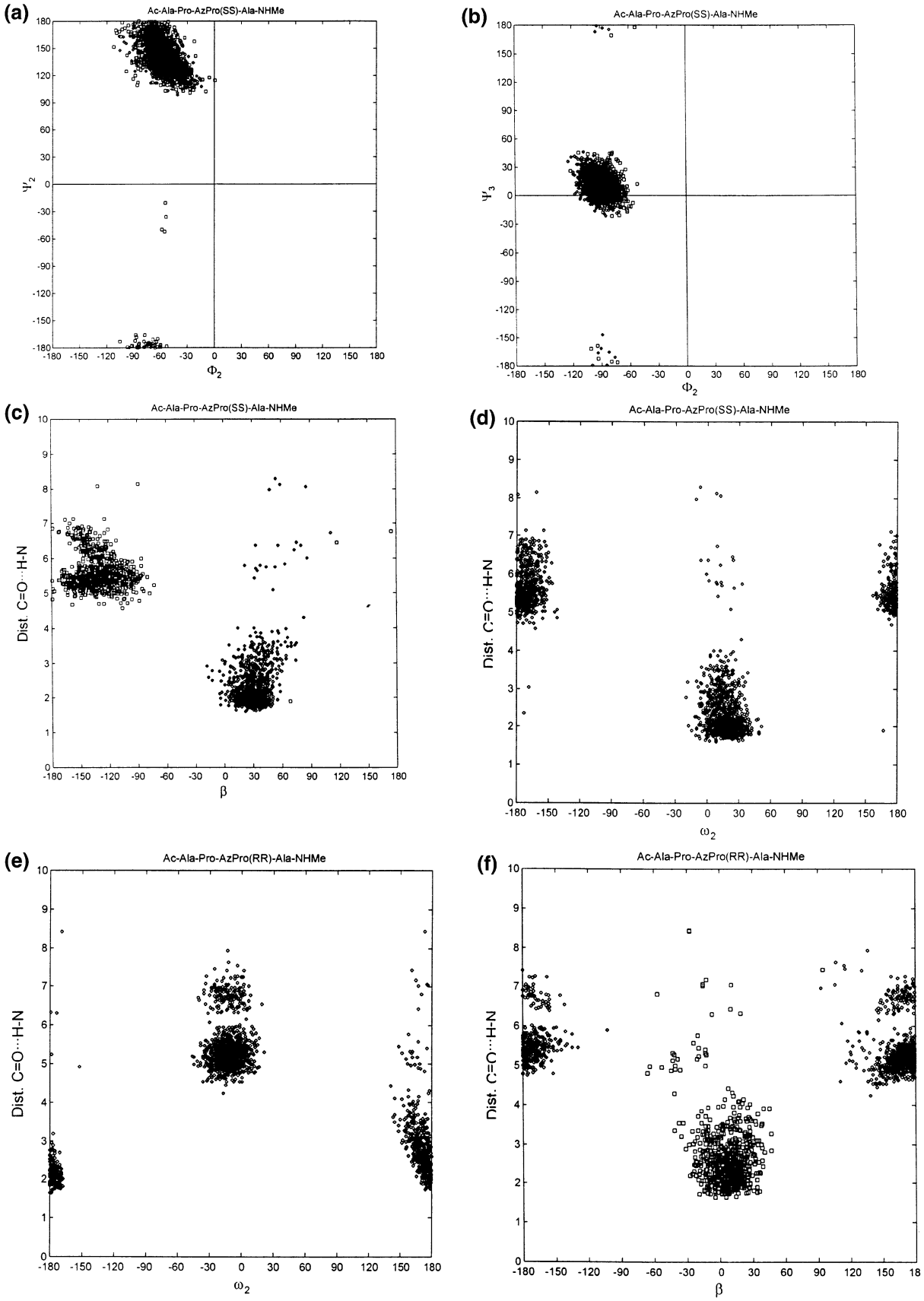

Figure 6. Results from the MC/SD simulations for Ac-Ala-Pro-azPro-Ala-NHMe. ◇ − Structures with a *cis*-amide bond; ◆ − structures with a *trans*-amide bond. (a) Ψ_2 vs Φ_2 for Ac-Ala-Pro-azPro(*S*,*S*)-Ala-NHMe. (b) Ψ_3 vs Φ_3 for Ac-Ala-Pro-azPro(*S*,*S*)-Ala-NHMe. (c) Hydrogen bond distance vs the virtual torsion β for Ac-Ala-Pro-azPro(*S*,*S*)-Ala-NHMe. (d) Hydrogen bond distance vs ω_2 for Ac-Ala-Pro-azPro(*S*,*S*)-Ala-NHMe. (e) Hydrogen bond distance vs ω_2 for Ac-Ala-Pro-azPro(*R*,*R*)-Ala-NHMe. (f) Hydrogen bond distance vs the virtual torsion β for Ac-Ala-Pro-azPro(*R*,*R*)-Ala-NHMe.

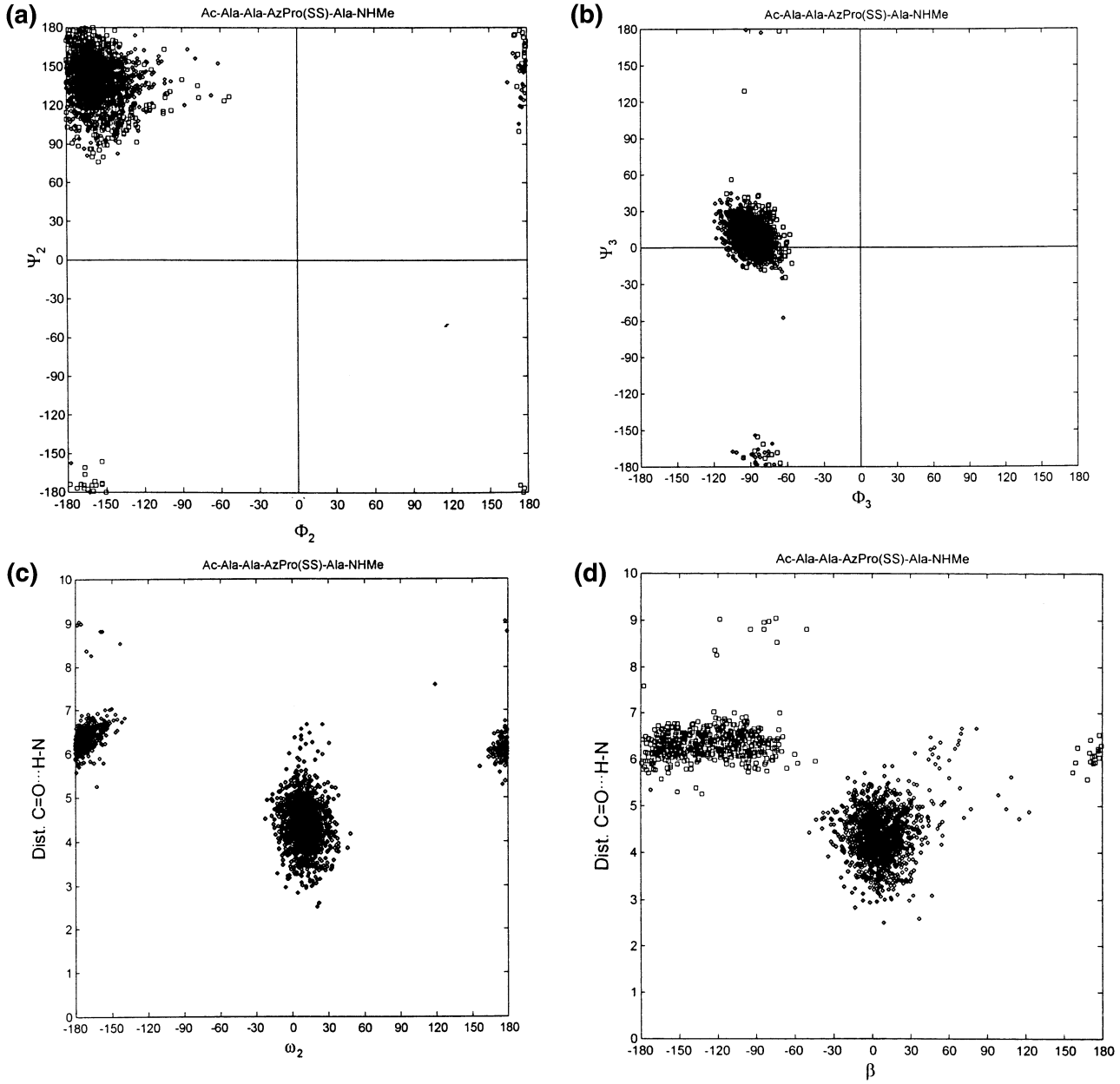

Figure 7. Results from the MC/SD simulations for Ac-Ala-Ala-azPro-Ala-NHMe. ◇ − Structures with a *cis*-amide bond; ◆ − structures with a *trans*-amide bond. (a) Ψ_2 vs Φ_2 for Ac-Ala-Ala-azPro(*S*,*S*)-Ala-NHMe. (b) Ψ_3 vs Φ_3 for Ac-Ala-Ala-azPro(*S*,*S*)-Ala-NHMe. (c) Hydrogen bond distance vs ω_2 for Ac-Ala-Ala-azPro(*S*,*S*)-Ala-NHMe. (d) Hydrogen bond distance vs the virtual torsion β for Ac-Ala-Ala-azPro(*S*,*S*)-Ala-NHMe.

Boc-Ala-azPro(*R*,*R*)-Ala-NHiPr and Boc-Ala-azPro(*S*,*S*)-Ala-NHiPr. Because these are tripeptides, the measurements had to be modified. For the virtual torsion angle, the ester oxygen −O− was used instead of the Cα1; the same thing was done for the Cα1−Cα4 distance where the ester oxygen was used instead of Cα4. For internal hydrogen bonding, the carbonyl oxygen on the Boc-group was used instead of the carbonyl oxygen for the first residue. The same tendency is seen for this peptide as the ones mentioned above; the *S*,*S* conformation is the diastereomer that forms a reverse turn more easily. 72.7% of the *S*,*S* conformations from the MD/SD run have a *cis*-conformation for the central amide bond. The conformations are similar to those in the MD/SC run for the tetrapeptide with alanines, Ac-Ala-Ala-azPro-Ala-NHMe. The Φ and Ψ plots (Figure 8a,b) show that there is no difference in Φ and Ψ space between the *cis*- and *trans*-conformations. It can also be seen that most of the conformations have the type VIb β-turn, but there is also a small cluster of conformations that have a type VIa β-turn. Figure 8c, hydrogen bond distance versus ω_2, shows that a *cis*-conformations are required to give a hydrogen bond. The figure also reveals that few of the conformations have a strong hydrogen bond; only 3.5% of the conformations have a distance of less than 2.5 Å between the carbonyl oxygen and the amide hydrogen. The *R*,*R* diastereomer showed the same behavior as that of the previous *R*,*R* diastereomer.

Boc-Ala-azPro(*R*,*R*)-D-Ala-NHiPr and Boc-Ala-azPro(*S*,*S*)-D-Ala-NHiPr. Table 3 shows that the Boc-Ala-azPro(*S*,*S*)-D-Ala-NHiPr has the highest degree of *cis*-amide bond for all of the peptides in this study, 99%. Also in the virtual torsion angle and Cα1−Cα4 parameters, it has high values, 71.5 and 77.1%, respectively. The Φ and Ψ plots (Figure 9a,b) show that the spread in Φ_2 and Ψ_2 is greater than that for the other

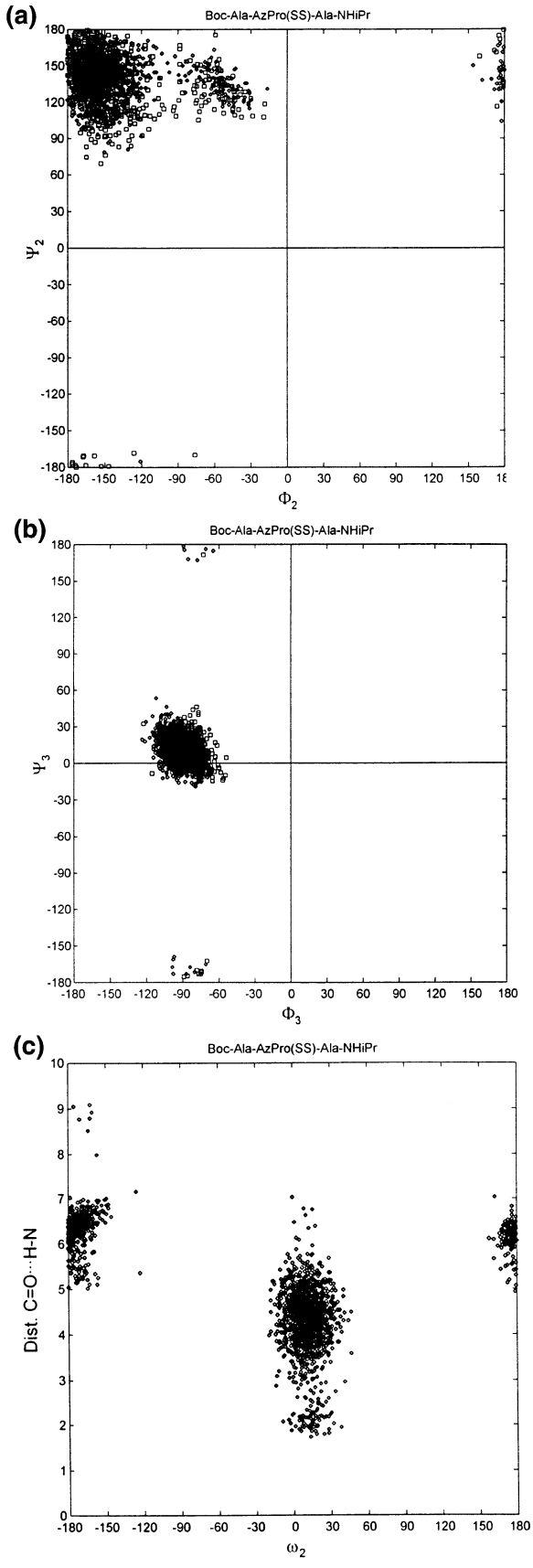

Figure 8. Results from the MC/SD simulations for Boc-Ala-azPro-Ala-NHiPr tripeptide. ◇ − Structures with a *cis*-amide bond; ◆ − structures with a *trans*-amide bond. (a) Ψ_2 vs Φ_2 for Boc-Ala-azPro(*S*,*S*)-Ala-NHiPr. (b) Ψ_3 vs Φ_3 for Boc-Ala-azPro(*S*,*S*)-Ala-NHiPr. (c) Hydrogen bond distance vs ω_2 for Boc-Ala-azPro(*S*,*S*)-Ala-NHiPr.

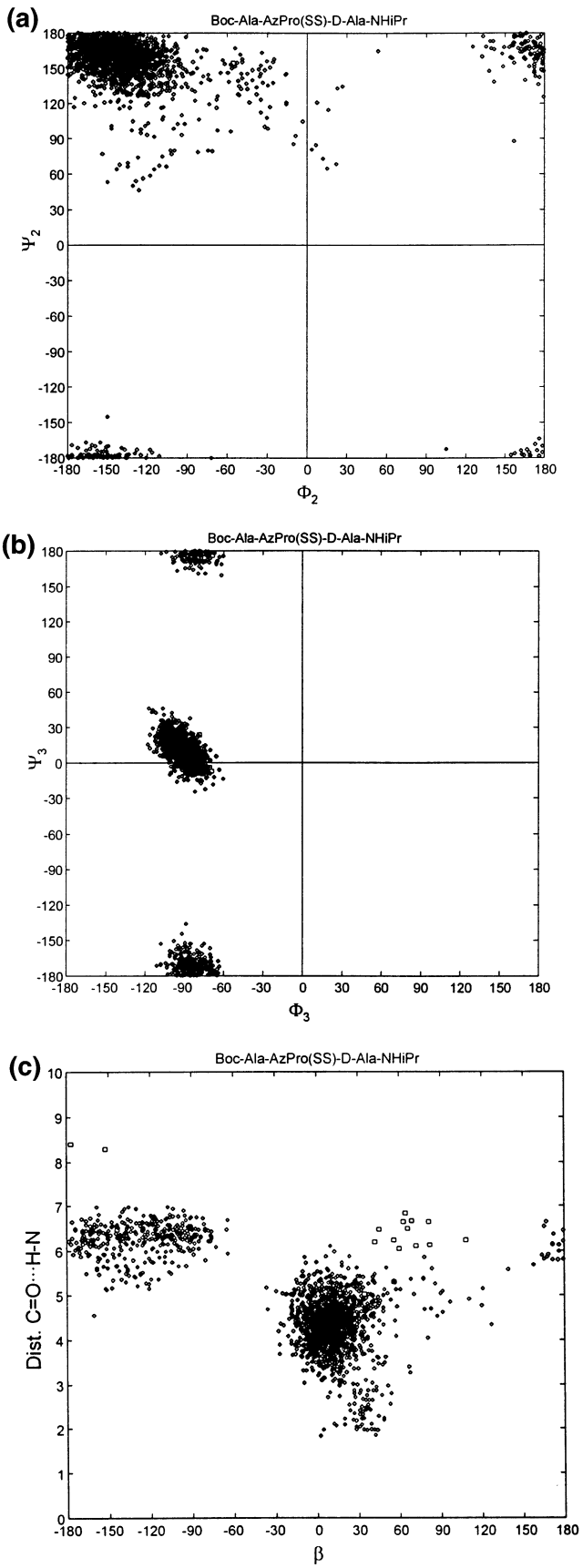

Figure 9. Results from the MC/SD simulations for Boc-Ala-azPro-D-Ala-NHiPr tripeptide. ◇ − Structures with a *cis*-amide bond; ◆ − structures with a *trans*-amide bond. (a) Ψ_2 vs Φ_2 for Boc-Ala-azPro(*S*,*S*)-D-Ala-NHiPr. (b) Ψ_3 vs Φ_3 for Boc-Ala-azPro(*S*,*S*)-D-Ala-NHiPr. (c) Hydrogen bond distance vs the virtual torsion β for Boc-Ala-azPro(*S*,*S*)-D-Ala-NHiPr.

peptides. The Φ_3 versus Ψ_3 plot, Figure 9a, shows two distinctive clusters, one around $\Phi_3 = -90°$, $\Psi_3 = 0°$ and the other cluster around $\Phi_3 = -90°$ and $\Psi_3 = -180°$. 20.8% of the conformations have a hydrogen bond distance less than 4 Å, while only 3.5% are within 2.5 Å. This indicates that the structures are not stabilized with an internal hydrogen bond. Figure 9c shows that the *cis*-conformations can form both a reversed turn with the virtual torsion around zero and also extended conformations with a virtual torsion larger than 90°. This is a bit unexpected because it is usually the *trans*-conformation that has the less tight turn, as can be seen for the peptides discussed above. The *cis*-conformation seems to be the far more stable conformation independent of the other torsion angles whether it forms a reverse turn or not. These findings are also true for the *R*,*R* diastereomer, even though the degree of reverse turns in the conformations from the MD/SD simulations is less, as can be seen from Table 3.

Conclusions

In the search for a new type VI β-turn-inducer, azaproline was of significant interest on the basis of initial crystal structures and NMR studies in organic solvent. As compared to many other types of type VI β-turn inducers, azPro makes only a small change to the overall geometry and conformation of proline and does not introduce additional steric bulk that could compromise receptor interactions. Conformational searches and MD/SD simulations using the GB/SA solvation model indicated that an azaproline increases the propensity for a *cis*-conformation in the amide bond preceding the azPro and, by formation of that *cis*-amide, the likelihood for a type VI β-turn. The results from MD/SD simulation for the Ac-Ala-Pro-azPro-Ala-NHMe tetrapeptide showed an increased degree of type VIa β-turn, with more than 50% of the conformations having a *cis*-amide bond and also a high degree of internal hydrogen bonding. Changing the second residue to an alanine resulted in a slightly different type of β-turn. The results for Ac-Ala-Ala-azPro-Ala-NHMe also show the same trend in the degree of reverse turn, but it is closer to a type VIb β-turn with no stabilizing internal hydrogen bond. The conformational searches revealed that the *cis*-conformation is the most stable for all of the tetrapeptides with an azaproline, ranging from 0.5 to 4.6 kJ/mol more stable than the *trans*-conformation. Also, the tripeptides studied earlier by Boussard et al.[67] showed the same behavior, a high degree of reverse turn.

The calculations for TRH and [azPro^3]-TRH did not generate the same results as the calculations for the tetrapeptides, or the experimental studies, supporting enhanced *cis*-conformational stability. In conformational searches, the *trans*-conformation was the most stable conformation for both TRH and [azPro^3]-TRH. The higher stability of the *trans*-conformation is likely to come from the interaction between the carboxamide and the His^2-imidazole ring. This hydrogen-bonding interaction, only possible with a *trans*-amide bond, favors the *trans*-amide bond over the *cis*-amide bond. Changing the imidazole group to a phenyl ring removed the possibilities of this interaction, with results on relative stabilities of *cis*−*trans*-amide conformers similar to the results from the calculations for [Phe^2, azPro^3]-TRH as compared with [azPro^3]-TRH.

The biological activity of the two analogues of TRH containing azPro are perfectly consistent when compared with TRH and [Phe^2]-TRH. The enhanced relative activity of TRH may be due, in part, to the conformation seen when the imidazole ring is hydrogen bonded to the backbone.[71] This was supported by studies of 6-(1-methylhistidine) and 6-(3-methylhistidine) analogues of TRH by Rivier et al.,[72] where [3-MeHis^2]-TRH had 8-fold enhanced activity as compared to that of TRH, and [1-MeHis^2]-TRH was essentially inactive.

One problem with azPro is that the two hydrazine nitrogens have a prochiral motif; they are either *R*,*R* or *S*,*S*. Both diastereomers were explicitly used in these studies because the nitrogens can readily invert at room temperature between these two diastereomers. For most of the examples, the two diastereomers give similar results in the MD/SD simulations, but, for example, in [azPro^3]-TRH, the differences are larger.

Acknowledgment. We acknowledge the National Institutes of Health (GM 53630) for partial support of this research as well as a postdoctoral fellowship (A.B.) from the Knut and Alice Wallenberg Foundation. The Washington University Mass Spectroscopy Resource Center partially supported by NIH (RR00954) and the Washington University High Resolution NMR Resource Center (NIH RR02004, RR05018 and RR07155) were utilized to characterize the peptide analogues synthesized as part of this study.

JA020994O

(71) Grant, G.; Ling, N.; Rivier, J.; Vale, W. *Biochemistry* **1972**, *11*, 3070−3073.
(72) Rivier, J.; Vale, W.; Monahan, M.; Ling, N.; Burgus, R. *J. Med. Chem.* **1972**, *15*, 479−482.